Major article

Redistribution of the novel *C. difficile* spore-adherence receptor, E-cadherin, by TcdA and TcdB increases spore-binding to adherens junctions.

Pablo Castro-Córdova[1,#,$], Macarena Otto-Medina[2,#], Nicolás Montes-Bravo[1,#], Christian Brito-Silva[1], D. Borden Lacy[3], Daniel Paredes-Sabja [1,4]*

[#] Authors contributed equally to this work.

[1] ANID – Millennium Science Initiative Program – Millennium Nucleus in the Biology of the Intestinal Microbiota, Santiago, Chile.

[2].Departamento de Ciencias Biológicas, Facultad de Ciencias de la Vida, Universidad Andrés Bello, Santiago, Chile.

[3] Department of Pathology, Microbiology, and Immunology, Vanderbilt University School of Medicine, Nashville, Tennessee, USA.

[4] Department of Biology, Texas A&M University, College Station, Texas, USA.

[$]Present address: IMPACT, Center of Interventional Medicine for Precision and Advanced Cellular Therapy, Santiago, Chile.

Short Title: Association of *C. difficile* spores to adherens junctions.

Key words*: C. difficile* spores, E-cadherin, adherens junctions

*Corresponding Author. Dr. Daniel Paredes-Sabja, Department of Biology, Texas A&M University, College Station, TX, 77843, USA. E-mail: dparedes-sabja@bio.tamu.edu

Word Count

Abstract: 167 words

Text (introduction, methods, results, and discussion): 3493 words

References: 50

ABSTRACT

Clostridioides difficile causes antibiotic-associated diseases in humans ranging from mild diarrhea to severe pseudomembranous colitis and death. A major clinical challenge is the prevention of disease recurrence, which affects nearly ~20 to 30 % of the patients with a primary *C. difficile* infection (CDI). During CDI, *C. difficile* forms metabolically dormant spores that are essential for recurrence of CDI (R-CDI). In prior studies, we have shown that *C. difficile* spores interact with intestinal epithelial cells (IECs), which contributes to R-CDI. However, this interaction remains poorly understood. Here, we provide evidence that *C. difficile* spores interact with E-cadherin, contributing to spore-adherence and internalization into IECs. *C. difficile* toxins TcdA/TcdB lead to adherens junctions opening and increase spore-adherence to IECs. Confocal micrographs demonstrate that *C. difficile* spores associate with accessible E-cadherin; spore-E-cadherin association increases upon TcdA/TcdB intoxication. The presence of anti-E-cadherin antibodies decreased spore adherence and entry into IECs. By ELISA, immunofluorescence, and immunogold labelling, we observed that E-cadherin binds to *C. difficile* spores, specifically to the hair-like projections of the spore, reducing spore-adherence to IECs. Overall, these results expand our knowledge of how *C. difficile* spores bind to IECs by providing evidence that E-cadherin acts as a spore-adherence receptor to IECs and by revealing how toxin-mediated damage affects spore interactions with IECs.

Key Words:

C. difficile spores, E-cadherin, spore-host interaction, *C. difficile* toxins TcdA/TcdB.

52 **INTRODUCTION**

53 *C. difficile* is a Gram-positive, anaerobic, spore-forming bacterium and the main causative
54 agent of antibiotic-associated diarrhea, causing death in ~5% of cases (1, 2). R-CDI is a major
55 clinical challenge affecting ~30% of CDI patients (2, 3). CDI is primarily driven by the *C. difficile*
56 toxins TcdA and TcdB, with contributions from the binary transferase toxin in some cases (4-6).
57 Both TcdA and TcdB target their intracellular glucosyltransferase activity towards RhoA, Rac1,
58 and Cdc42 (7, 8). This inhibitory modification of the Rho GTPase family leads to actin
59 depolymerization and disruption of tight and adherens junctions (9-13), causing disruption of
60 epithelial paracellular barrier function (14). Clinical studies showed that administration of anti-
61 TcdB antibody (bezlotoxumab) in combination with antibiotics reduces R-CDI rates (15). The
62 antibody may prevent toxin-mediated stem cell dysfunction and therefore prevent the delay in
63 recovery and repair of the intestinal epithelium (10).

64

65 During infection, *C. difficile* produces spores (16). Strains unable to form spores do not
66 cause R-CDI in animal models (17), indicating that the spores are critical for R-CDI. EDTA-
67 disruption of cell-cell junctions in Caco-2 cells leads to increased adherence of *C. difficile* spores
68 at the cell-cell junction, suggesting a tropism for cell-cell junctions (18). *C. difficile* spores bind to
69 fibronectin and vitronectin, located in the basolateral membrane (19). These molecules contribute
70 to *C. difficile* spore internalization into IECs in an integrin-dependent manner, and spore-entry *in*
71 *vivo* contributes to the R-CDI (20).

72

73 The intestinal barrier is an impermeable layer that separates the apical and basolateral cell
74 sides (21), and is formed by junctions between adjacent IECs. The cell-cell junctions between IECs

are constituted of E-cadherin containing adherens junctions and tight junctions formed by claudins, occludins, and zonula occludens. These junctions provide the gut barrier with impermeability properties and restrict the translocation of pathogens and commensal bacteria. However, some pathogens can alter or disrupt the cell junctions, to translocate through the host (22).

Several enteric pathogens such as *Streptococcus pneumoniae*, *Fusobacterium nucleatum*, *Campylobacter jejuni*, and *Listeria monocytogenes* take advantage of disrupted intestinal adherens junctions to internalize in host cells (23-27). How *C. difficile* spores interact with adherens junctions remains poorly described. Herein, we show that accessible E-cadherin is reduced in differentiated Caco-2 cells. Also, TcdA/TcdB intoxication increases the spore adherence that is correlated with an increase in E-cadherin accessibility in IECs. Next, we observed that *C. difficile* spores interact with E-cadherin in healthy IECs and the binding is increased in TcdA/TcdB-intoxicated cells. Also, the blocking of the cellular E-cadherin with monoclonal antibodies reduces the spore adherence and entry to IECs. Finally, we observed that E-cadherin binds to the hair-like extensions of the exosporium.

METHODS

Bacterial growth conditions.

C. difficile was grown under anaerobic conditions at 37 °C in a Bactron III–2 chamber (Shellab, OR, USA) in BHIS medium; 3.7% brain–heart infusion broth (BD, USA) supplemented with 0.5% of yeast extract (BD, USA), and 0.1% L–cysteine (Merk, USA) liquid or on plates with 1.5% agar (BD, USA). *C. difficile* strain R20291 wild-type B1/NAP1/PCR-ribotype 027 strain obtained from CRG0825 stock at Nottingham Clostridia Research Group (28). *C. difficile*

98 630Δ*erm* is a toxigenic (*tcdA*$^+$ *tcdB*$^+$) strain of *C. difficile* isolates from a patient with
99 pseudomembranous colitis during an outbreak of CDI (29). *C. difficile* 630Δ*erm bclA1::CT*,
100 630Δ*erm bclA2::CT* and 630Δ*erm bclA3::CT* are insertional inactivation clostron mutant strains
101 in the exosporium collagen-like proteins BclA1, BclA2 and BclA3 (30), and were a kind gift from
102 Dr. Simon Cutting (School of Biological Sciences, Royal Holloway, University of London).
103 *Bacillus megaterium* transformed with the plasmid pHIS 1622 that contains the cloned genes *tcdA*
104 and *tcdB* of *C. difficile* VPI 10463 (31), were aerobically grown at 37 °C in Luria-Bertani (BD)
105 with 10 µg/mL tetracycline.
106
107 **Cell lines and culture conditions**
108 Caco-2 cells (ATCC, USA) were grown at 37 °C with 5% CO_2 with Dulbecco's modified
109 Eagle's minimal essential medium High Glucose (DMEM; Hyclone, USA) supplemented with
110 10% of fetal bovine serum (FBS; Hyclone, USA) and 50 U mL^{-1} penicillin, and 50 µg mL^{-1}
111 streptomycin (Corning Cellgro, USA) as previously has been described For experiments, cells
112 were plated over glass coverslips in 24–well plates and were cultured for 2–days post–confluence
113 (undifferentiated) or 8–days post–confluence (differentiated), changing the media every other day.
114 To polarize Caco-2 cells were cultured onto 12mm Transwell (Corning, USA) with pores size of
115 0.4 µm until transepithelial electric resistance >250 Ω × cm^2.
116
117 **Recombinant *C. difficile* toxin Purification**
118 *C. difficile* toxins, TcdA and TcdB, were expressed in *B. megaterium* transformed with the
119 plasmid pHIS1622, containing the cloned genes *tcdA* and *tcdB* of *C. difficile* VPI 10463 as
120 previously described (31). Briefly, transformed *B. megaterium* were cultured in Luria–Bertani

121 medium (BD, USA) supplemented with 10 μg mL^{-1} tetracycline, and 35 mL of an overnight
122 culture was used to inoculate 1L of media. Bacteria were grown at 37 °C with 220 rpm. Toxin
123 expression was induced with 0.5% D–xylose once the culture reached OD_{600} = 0.5. Cells were
124 harvested after 4 h by centrifugation at 4,750×*g* and resuspended in 200 mL of binding buffer (20
125 mM Tris [pH 8.0], 100 mM NaCl for TcdA and 20 mM Tris [pH 8.0], 500 mM NaCl for TcdB)
126 supplemented with 0.16 μg mL^{-1} DNase, 10 mg mL^{-1} lysozyme and protease inhibitors (P8849;
127 Sigma). Cell lysis was performed using an Emulsiflex homogenizer, and lysates were centrifuged
128 at 48,000×*g* for 30 min. The toxins were purified from the supernatant by Nickel–affinity, anion
129 exchange, and size–exclusion chromatography. Toxins were eluted and stored in 20 mM HEPES
130 (pH 7.0), 50 mM NaCl.
131
132 **Spore preparation and purification**
133 *C. difficile* spores were purified as we previously described (32). Briefly, *C. difficile* spore
134 was cultured overnight in BHI medium in a Bactron III–2 anaerobic chamber (Shellab, USA).
135 Then a 1:500 dilution was plated in TY agar plates; 3% trypticase soy and 0.5% yeast extract and
136 1.5% Bacto agar (BD, USA) and incubated for 7 days at 37 °C in anaerobiosis. Colonies were
137 harvested with sterile, cold Milli–Q water, washed 3 times and purified with 50% Nicodenz. The
138 spore suspension was 99% free of vegetative cells, sporulating cells, and debris. Spores were
139 quantified in a Neubauer chamber and stored at –80 °C until use.
140
141 **Immunofluorescence of cell monolayers.**
142 To evaluate E-cadherin distribution in undifferentiated and differentiated Caco-2 cells,
143 cells were washed with PBS and were fixed with PBS–4% paraformaldehyde for 20 min at 4 °C,

144 blocked with PBS–3% BSA 1 h at room temperature (RT). To stain the accessible E-cadherin,
145 cells were incubated with 1: 50 of primary antibody mouse polyclonal anti–human E-cadherin (sc-
146 8426, Santa Cruz Biotechnology, USA) in PBS–3% BSA, for 2 h at RT followed by two washed
147 with PBS and 1:200 secondary antibody donkey anti–mouse-Alexa Fluor 568 (ab175700, Abcam,
148 USA). To detect the total E-cadherin, fixed samples were permeabilized with PBS-0.2% Triton
149 100-X for 10 min at RT and blocked with PBS–3% BSA for 1 h at RT. The total protein was
150 detected with the same primary antibody used accessible E-cadherin; primary antibody mouse
151 polyclonal anti–human E-cadherin (sc-8426, Santa Cruz Biotechnology, USA) in PBS–3% BSA
152 that was incubated for 2 h at RT, then were washed and was incubated with 1:200 secondary
153 antibody donkey anti–mouse-Alexa Fluor 568 (ab175700, Abcam, USA). The non–permeabilized
154 samples stained for accessible E-cadherin were permeabilized with PBS-0.2% Triton 100-X for
155 10 min at RT, washed, and to stain the F–actin, cells were incubated with 1:1,000 Phalloidin i–
156 Fluor 488 (ab176753, Abcam, USA) in PBS for 30 min at RT. Cells were washed, and nuclei were
157 stained with 8 μg mL^{-1} Hoechst 33342 (ThermoFisher, USA) in PBS for 10 min at RT. Then
158 samples were washed and mounted using Dako Fluorescent Mounting Medium (Dako, Denmark).
159 Samples were visualized in the confocal microscope Leica TCS LSI (Leica, Germany). Please see
160 below.
161
162 To study the redistribution of E-cadherin in TcdA/TcdB intoxicated cells, differentiated
163 Caco-2 cells cultured into 24–well plates were washed twice with DPBS (Hyclone, USA) and were
164 intoxicated with 600 pM TcdA and 600 pM TcdB for 3, 6, and 8 h in DMEM, without serum. As
165 a control, cells were incubated in the same solution without TcdA/TcdB. Then cells were rinsed
166 with PBS, fixed with PBS–4% paraformaldehyde, and washed with PBS and blocked with PBS–

167 1% BSA at 4 °C overnight. To stain the surface, accessible E-cadherin cells were incubated with
168 1:200 mouse mAb anti–E-cadherin (SC8426, Santa Cruz Biotechnologies, USA), 1 h at RT,
169 washed, and followed incubation with 1:400 donkey anti–mouse IgG Alexa Fluor 488 (ab150109,
170 Abcam, USA) for 1 h at RT. To detect the total protein, samples were permeabilized with PBS–
171 0.2% Triton 100-X for 10 min at RT and blocked with PBS–1% BSA for 1 h at RT. The total
172 protein was detected with the same primary antibody used before, washed, and samples were
173 incubated with donkey anti–mouse IgG Alexa Fluor 568 (ab175700, Abcam, USA). Samples were
174 mounted using Dako Fluorescent Mounting Medium (Dako, Denmark) and were visualized in the
175 confocal microscope Leica Sp8 (Leica, Germany; please see below.)
176
177 To evaluate *C. difficile* spore association with accessible E-cadherin in TcdA/TcdB
178 intoxicated IECs, differentiated Caco-2 cells were intoxicated with 600 pM TcdA and 600 pM
179 TcdB for 8 h at RT, as described above. Then cells were infected with *C. difficile* spores in an MOI
180 of 10 for 1 h at 37 °C. Then cells were washed, fixed with PBS–4% paraformaldehyde for 10 min
181 at RT, blocked with PBS–1% BSA overnight at 4 °C, and *C. difficile* spores were stained with
182 1:1,000 primary polyclonal anti–*C. difficile* spore IgY batch 7246 antibodies (33) (Aveslab, USA)
183 in PBS–1% BSA for 1 h at RT. Following two PBS washed, samples were incubated with 1:400
184 goat anti–chicken IgY secondary antibodies Alexa–Fluor 488 (#ab150173 Abcam, USA) in PBS–
185 3% BSA for 1 h at RT, washed two times with PBS, and accessible E–cadherin was stained as it
186 is described above. Cellular nuclei were stained with 8 μg mL^{-1} Hoechst 33342 (ThermoFisher,
187 USA) for 15 min at RT. Finally, samples were mounted and analyzed by confocal microscopy
188 Leica SP8.
189

190 The Leica microscopes TCS LSI and SP8 at the Confocal Microscopy Core Facility of the
191 Universidad Andrés Bello were used. To evaluate E-cadherin distribution in undifferentiated and
192 differentiated Caco-2 cells, Leica TCS LSI was used with 63× ACS APO oil objective numerical
193 aperture 1.3, with an optical zoom of 2×. Micrographs were acquired using excitation wavelengths
194 of 405, 488, and 532 nm, and signals were detected with an ultra–high dynamic photomultiplier
195 (PMT) spectral detector (430–750nm). Emitted fluorescence was split with four dichroic mirrors
196 (QD 405, 488, 561, and 635 nm). Images 1,024 × 1,024 pixels were acquired each 0.3 µm. To
197 observe the redistribution of accessible E-cadherin and total E-cadherin in TcdA and TcdB
198 intoxicated cells, Leica SP8 was used with HPL APO CS2 40× oil, numerical aperture 1.30. For
199 signal detection, three PMT spectral detectors were used; PMT1 (410–483) DAPI, PMT2 (505–
200 550), Alexa–Fluor 488, and PMT3 (587–726) Alexa–Fluor 555. Emitted fluorescence was split
201 with dichroic mirrors DD488/552. Pictures of 1,024 × 1,024 pixels were captured each 0.3 µm.
202 Images of 3–dimensional reconstructions of the Caco-2 monolayers were performed using ImageJ
203 software (NIH, USA). In undifferentiated and differentiated cells, accessible E-cadherin cells were
204 quantified as the number of cells with positives staining. To quantify the redistribution of E-
205 cadherin, Fl. Int. of each slide was measured using the plug–in "Measure stack" of Fiji (ImageJ,
206 NHI, USA), and the sum of the Fl. Int. of each slide is considered as the Fl. Int. of the *z*–stack of
207 a field for accessible and total E-cadherin. For each field, the same number of slides was used.
208

209 **Quantification of *C. difficile* spore adherence and internalization.**

210 To evaluate spore adherence and internalization in TcdA/TcdB intoxicated cells,
211 differentiated Caco-2 cells were incubated with 600 pM TcdA and 600 pM TcdB for 3, 6, and 8 h
212 in DMEM, without serum. As a control, cells were incubated in the same solution without

213 TcdA/TcdB or cells were incubated with TcdA/TcdB previously heat inactivated at 70°C for 5
214 min. Then cells were infected with *C. difficile* spores an MOI 10 for 3 h at 37 °C. Unbound spores
215 were rinsed off with PBS, and cells were fixed with PBS–4% paraformaldehyde for 10 min, and
216 adhered spores were stained as described below.
217
218 To evaluate spore adherence and entry in presence of anti–E-cadherin, undifferentiated,
219 differentiated, and polarized Caco-2 cells were incubated with 0,1; 1,0; 10; 100 µg mL^{-1} of mouse
220 monoclonal anti–human E-cadherin (SC8426, Santa Cruz Biotechnology, USA) or as control non–
221 immune IgG antibody of rabbit serum (I5006, Sigma-Aldrich, USA) for 2 h at 37 °C. Then cells
222 were infected for 3 h at 37 °C with *C. difficile* spores, previously incubated with 20 µL of FBS per
223 well for 1 h at 37 °C. Cells were washed two times with PBS to remove unbound spores and were
224 fixed with PBS–4% paraformaldehyde for 10 min at RT, and adhered spores were stained as
225 described below.
226
227 To evaluate spore adherence and entry in presence of purified E-cadherin, undifferentiated
228 and differentiated Caco-2 cells were infected with *C. difficile* spores previously incubated with 1,
229 2.5, 5, 10 and 25µg mL^{-1} of human purified E-cadherin (5085, Sigma-Aldrich, USA) in DMEM
230 or DMEM without FBS as control for 1 h at 37 °C. Then cells were infected and were incubated
231 for 3 h at 37 °C. Cells were washed two times with PBS to remove unbound spores, fixed with
232 PBS–4% paraformaldehyde for 10 min at RT, and adhered spores were stained as described below.
233
234 To evaluate whether the presence of E-cadherin decreases the spore adherence in
235 TcdA/TcdB intoxicated cells, undifferentiated and differentiated Caco-2 cells were 8 h-

236 TcdA/TcdB intoxicated and were infected for 1 h at 37 °C with *C. difficile* spores previously
237 incubated with 25 μg mL^{-1} of E-cadherin for 1 h at 37 °C. Cells were washed two times with PBS
238 to remove unbound spores, fixed with PBS–4% paraformaldehyde for 10 min at RT, and adhered
239 spores were stained as described below.
240
241 In undifferentiated, differentiated, and polarized *C. difficile* spore infected Caco-2 cells,
242 adhered *C. difficile* spores were immunostained using the intracellular spore exclusion
243 immunostaining assay as previously described (20). For this *C. difficile* spore–infected cells were
244 washed three times with PBS at RT, blocked with PBS–3% BSA overnight at 4 °C, and samples
245 were incubated with anti–*C. difficile* spore goat serum 1:50 (PAC 5573, Pacific Immunology,
246 USA) in PBS–1% BSA for 1 h at RT. The cells were washed 3 times with PBS and incubated with
247 1:400 secondary antibody donkey IgG anti–goat CFL 488 (SC362255, Santa Cruz Biotechnology,
248 USA) for 1 h at RT. Cells were washed, and DNA was stained with 8 μg mL^{-1} Hoechst 33342
249 (ThermoFisher, USA) for 15 min at RT. In the case of polarized cells, to stain the F–actin, samples
250 were incubated with 1:100 Phalloidin Alexa Fluor 568 (A12380, Invitrogen, USA) for 30 min at
251 RT. Samples were washed three times with PBS and one time with distilled water and mounted
252 with Dako Fluorescent Mounting Medium (Dako, Denmark). Samples were visualized in the
253 epifluorescence microscope Olympus BX53 fluorescence microscopy with UPLFLN 100× oil
254 objective (numerical aperture 1.30). Images were captured with the camera for fluorescence
255 imaging Qimaging R6 Retiga, and pictures were analyzed with ImageJ (NIH, USA). Adhered
256 spores were considered as spores in phase–contrast that were marked in fluorescence. Internalized
257 spores were considered spores in phase–contrast, but that do not have fluorescence. In the case of

258 polarized cells, it was only possible to quantify adhered spores. The number or adhered spores
259 were quantified, and data were normalized to the control.
260
261 **ELISA of E-cadherin bound to *C. difficile* spores.**
262 Ninety six-well plate were coated overnight at 4ºC with 100 µL/well containing 1.6 x 10^8
263 spores mL^{-1} or with 100 µL of PBS containing 1 µg of BSA in PBS (as a control). overnight at 4
264 °C. Wells were washed 5 times with PBS–0.05% Tween-20 (PBS–Tween) to remove unbound
265 spores and blocked with 200 µL of PBS–Tween–2% BSA (Sigma Aldrich, USA) for 1 h at 37 °C.
266 The spores were washed and incubated with 50 µL of 0.2, 2.0, 20, and 200 nM of recombinant
267 human purified E-cadherin (5085, Sigma-Aldrich, USA) for 1 h at 37 °C. Unbonded E-cadherin
268 was washed 5 times with 150 µL PBS–Tween and was incubated with 50 µL of 1:50 IgG of mouse
269 anti–E-cadherin (SC8426-Santa Cruz Biotechnology, USA) in PBS–Tween–1% BSA for 1 h at 37
270 °C. Wells were washed five times with PBS–Tween and then incubated with 50 µL of 1: 5,000
271 secondary antibody anti–mouse-HRP (610-1302, Rockland, USA) 1 h at 37 °C. Then, wells were
272 washed five times with PBS–Tween and once with carbonate buffer (pH 9.6). Finally, wells were
273 incubated with 50 µL of buffer substrate (17 mM citric acid, 65 mM potassium phosphate, 0.15%
274 hydrogen peroxide, and 0.4% θ-phenylenediamine) for 20 min at RT. The reaction was stopped
275 with 25 µL of 4.5 N H_2SO_4. The color intensity was quantified at 450 nm using the plate reader
276 Infinite F50, (Tecan, Switzerland).
277
278 **Immunofluorescence of E-cadherin bound to *C. difficile* spores.**
279 The immunofluorescence was performed as previously described with modification (19).
280 Briefly, 4 × 10^7 *C. difficile* spores were incubated with 1, 2.5, 5.0, 10, and 25 µg mL^{-1} of

281 recombinant human purified E-cadherin (5085, Sigma-Aldrich, USA) in PBS for 1 h at 37 °C.
282 Spores were washed 5 times with PBS and fixed with PBS–4% paraformaldehyde in poly–L-
283 lysine-treated 12 mm glass–coverslips (Marienfeld GmbH, Germany). The spores were washed 3
284 times with PBS and were blocked with PBS–3% BSA for 1 h at RT. Then, samples were incubated
285 with 1:50 mouse IgG anti–E-cadherin (SC8426, Santa Cruz Biotechnology, USA) for 2 h at RT
286 and washed 3 times with PBS and once with distilled H_2O. Finally, samples were mounted with
287 Dako Fluorescent Mounting Medium (Dako, Denmark), and images were captured in an
288 epifluorescence microscope Olympus BX53. The fluorescence intensity was quantified using Fiji
289 (ImageJ, NHI, USA). Data were normalized as $(\text{Fl. Int/area})_{\text{sample}} - (\text{Fl. Int/area})_{\text{background.}}$ The
290 Surface Plot was generated with the plug–in 3D surface Plot of Fiji (ImageJ, NHI, USA).
291
292 **SDS-PAGE and western blot of intoxicated Caco-2 cells.**
293 Undifferentiated and differentiated Caco-2 cells were intoxicated for 3, 6 and 8 h with TcdA/TcdB
294 in 24-well plates. The cells were washed and frozen at −80 °C. The frozen cells were lysed with
295 80 µL/well of cold RIPA buffer (50 mM Tris-HCl; 150 mM NaCl; 0.5% Deoxycholate; 1% NPO_4;
296 1mM EGTA; 1mM EDTA; 0.5% SDS; protease inhibitor) in ice and centrifuged at 18,400×*g* for
297 15 min at 4 °C. The supernatant was collected and 20 µg of protein was suspended in 2× SDS-
298 PAGE sample loading buffer, boiled and electrophoresed on 12% and 4% acrylamide SDS-PAGE
299 gels. Proteins were transferred to nitrocellulose membrane and blocked with 5% non-fat milk in
300 TBS for 1 h at RT. Membranes were probed for non-glucosylated Rac1 in Tris -buffered saline
301 containing 0.1% Tween (TTBS) with 5% milk and 1:1,000 mouse anti-Rac1 (Clone 102/Rac1
302 610650; BD Bioscience, USA) and then incubated overnight at RT and 6 h at RT. The membranes
303 were washed with TTBS and incubated with 1:5,000 goat anti-mouse HRP for 1 h at RT (Rockland

304 610-1302) in 5% milk-TTBS. Samples were washed 3 times with TTBS and HRP activity was
305 detected with a chemiluminescence detection system (Li-core) using PicoMax sensitive
306 chemiluminescence HRP substrate (Biorad, USA). To detect total Rac-1 in undifferentiated cells,
307 membranes were incubated twice with mild stripping solution (1.5% glycine, 0.1% SDS, 1%
308 Tween 20; pH 2.2) for 7 min at RT, washed twice with PBS and twice with TTBS 0.05%, and
309 blocked with 5% non-fat milk-TBS 1 h at RT. For differentiated cells, total Rac1 was detected in
310 the other membrane loaded simultaneously with the same concentration of protein. Membranes
311 were incubated with 1:1,000 mouse anti-Rac1 (clone 23A8 05-389; Merck Millipore, USA)
312 overnight at 4 °C and 3 h at RT and then washed 3 times with TTBS. Membranes were then
313 incubated with 1:5,000 goat anti-mouse HRP (Rockland 610-1302) 1 h at RT and washed 3 times
314 with TTBS. HRP activity was detected using Li-core as described for non-glucosylated Rac1.
315

316 **Transmission electron microscopy of E-cadherin bound to *C. difficile* spores.**

317 2.5×10^8 *C. difficile* spores were incubated with 10 µg mL^{-1} of recombinant human purified
318 E-cadherin (5085, Sigma-Aldrich, USA) with PBS for 1 h at 37 °C. Spores were washed 5 times
319 with PBS and centrifugation at 18,400×*g* for 5 min and were blocked with PBS–1% BSA for 20
320 min at RT. Then samples were incubated with 1:50 IgG of mouse anti–E-cadherin (SC8426, Santa
321 Cruz Biotechnologies, USA) in PBS–1% BSA for 1 h at RT, washed 3 times by centrifugation at
322 18,400×*g* for 5 min with PBS. Spores were incubated with IgG anti–mouse conjugated to 10nm
323 gold nanoparticles (G7777, Sigma-Aldrich, USA) for 1 h at RT. Then were washed 3 times with
324 PBS–0.1% BSA by centrifugation at 18,400×*g* for 5 min. Subsequently, spores were processes for
325 TEM, as previously have been described (19). Briefly, spores were fixed in 0.1 M cacodylate
326 buffer–2.5% glutaraldehyde with 1% paraformaldehyde and then fixed with 0.1 M cacodylate

327 buffer–1% osmium tetroxide and stained with 1% tannic acid for 30 min. Samples were dehydrated
328 with increasing acetone concentrations; 30% acetone (with 2% uranyl acetate only in this step) for
329 30 min, 50% acetone for 30 min, 70% acetone overnight, and 90% acetone for 30 min, and 2 times
330 with 100% acetone. Dehydrated samples were embedded in resin: acetone in a ratio of 3:1, 1:1,
331 and 1: 3 for 40 min each. Finally, samples were resuspended in resin for 4 h and incubated for 12
332 h at 65 °C. With a microtome, 90 nm sections cut and placed in a carbon–coated grid for negative
333 staining and double staining with 2% uranyl acetate with lead citrate. Sections were observed in a
334 transmission electron microscope Phillip Tecnai 12 bioTwin of the Pontificia Universidad Católica
335 de Chile. The distribution of thin or thick exosporium was quantified according to previously
336 described morphotypes (34).
337
338 **RESULTS**
339
340 **Characterization of accessible E-cadherin in monolayers of Caco-2 cells.** Caco-2 cells have
341 been employed to assess *C. difficile* interaction with IECs (18-20, 32, 33, 35-37). Early work
342 demonstrated that *C. difficile* spores had a tropism towards the cell-cell junction of EDTA-treated
343 Caco-2 cells (18). Therefore, to understand the dynamic of adherens junction closure during Caco-
344 2 cell differentiation, we assessed the accessibility of E-cadherin in undifferentiated and
345 differentiated monolayers of Caco-2 cells. First, Caco-2 cell differentiation was assessed for the
346 appearance of microvilli by TEM and sucrase-isomaltose as a differentiation marker in monolayers
347 cultured for 2- or 8-days post-confluency (19). Next, differentiated and undifferentiated Caco-2
348 cells were immunostained for accessible E-cadherin or permeabilized and stained for total E-
349 cadherin (Figure 1*A*, *B*). Results demonstrate that in undifferentiated Caco-2 cells, ~84% of the

350 cells were immunolabeled for accessible E-cadherin (Figure 1*C*), whereas, in differentiated Caco-
351 2 cells, only ~7% of the cells were stained for accessible E-cadherin (Figure 1*C*). As a control,
352 cells were permeabilized and stained for total E-cadherin, and we observed that ~100% of both
353 undifferentiated and differentiated Caco-2 cells were immunolabeled for E-cadherin (Figure 1*D-*
354 *F*). These results demonstrate that after 8-days of differentiation, most of the cells lack accessible
355 E-cadherin.
356
357 **Intoxication with *C. difficile* TcdA and TcdB increases accessible E-cadherin.** *C. difficile*
358 toxins TcdA and TcdB cause tight and adherens junction dissociation (9-11). TcdA, but not TcdB,
359 causes a displacement of E-cadherin from the cell-cell junctions to be located around the cells in
360 Caco-2 cells (11) while in colonic epithelium, TcdB causes adherens junctions disruption (10).
361 Since most of the *C. difficile* strains causing disease produces TcdA and TcdB (38), we asked
362 whether TcdA and TcdB affect the accessibility of E-cadherin in differentiated Caco-2 cells.
363 TcdA/TcdB-intoxicated differentiated Caco-2 cells for 3, 6, and 8 h were immunostained for
364 accessible E-cadherin (non-permeabilized) using an antibody that detects an extracellular domain
365 of E-cadherin, followed by fluorescent-labeled secondary antibody. For total E-cadherin staining,
366 cells were permeabilized and immunostained with the same primary antibody and a fluorescent-
367 labeled secondary antibody with another Alexa Fluor dye (See Methods). Then, we acquired
368 confocal micrographs, and the fluorescence intensity (Fl. Int.) was quantified for every slice of the
369 *z*-stack for accessible and total E-cadherin. The sum of the Fl. Int. of accessible E-cadherin was
370 significantly higher (175% relative to unintoxicated monolayers) after 8h-intoxication (Figure 2*A*,
371 *B*, Supplementary Figure 1). To evaluate if this increase of Fl. Int. occurs in the apical or basal half
372 of the monolayer, we split the number of slices of the z-stack into 2-halves (apical and basal) with

373 the same number of slices. We summed the Fl. Int. for accessible E-cadherin in the apical (Figure
374 2*C*) or basal (Figure 2*D*) halves of the monolayer. We observed a significant increase in accessible
375 E-cadherin Fl.Int. in both the apical and basal halves, 177% and 176% respectively, after 8h-
376 intoxication (Figure 2*C, D*). Using the same strategy, we quantified the total E-cadherin Fl. Int. in
377 the complete *z*-stack, and we observed a significant decrease of 19% after 6h- and an increase of
378 12.2% after 8h-intoxication compared to unintoxicated cells (Figure 2*E*). Then, we observed that
379 these variations were in the apical and not in the basal half of the monolayer. We observed a
380 decrease of 35% after 6h- and an increase of 44% after 8h-intoxication compared to unintoxicated
381 cells (Figure 2*F, G*). To confirm the degree of TcdA/TcdB intoxication, we evaluated the
382 glucosyltransferase activity by measuring the levels of glucosylated Rac1 in TcdA/TcdB
383 intoxicated differentiated and undifferentiated monolayers using strategies previously described
384 (39). After 3 h of intoxication no modification of Rac1 was observed. However, after 6 and 8 h of
385 intoxication, the unglucosylated Rac1 signal disappeared, indicating a complete glucosylation of
386 Rac1 (Figure 2*H*). These results indicate that the cells were fully intoxicated by 6 hours and
387 accessible E-cadherin is increased in differentiated Caco-2 cells after 8h-intoxication.
388
389 ***C. difficile* toxins TcdA and TcdB increase the adherence to IECs.** Several studies have shown
390 that vegetative *C. difficile*-adherence to IECs is enhanced following TcdA or CDT intoxication
391 (11, 40, 41). To expand the understanding of how intoxication of IECs impacts spore-adherence,
392 differentiated and undifferentiated Caco-2 cells were TcdA/TcdB intoxicated for 8 h, or incubated
393 8 h with heat inactivated TcdA/TcdB as a control. Then cells were washed and infected for 1 h
394 with *C. difficile* spores in the absence of serum. Cells were fixed and immunostained without
395 permeabilization. In TcdA/TcdB intoxicated Caco-2 cells, we observed more adhered spores

396 compared to unintoxicated cells (Figure 3*A*). After quantitative analysis, we observed in
397 undifferentiated Caco-2 cells that spore adherence in 8h-TcdA/TcdB-intoxicated cells was ~105%
398 higher than in unintoxicated monolayers, and no differences in spore adherence were observed in
399 cells 8 h-incubated with heat-inactivated TcdA/TcdB (Figure 3*B*). Similarly, in differentiated cells
400 we observed an increase in ~321% in 8 h-TcdA/TcdB-intoxicated cells over that in unintoxicated
401 monolayers, and no differences were observed in cells 8 h-incubated with heat-inactivated
402 TcdA/TcdB (Figure 3*C*). Collectively these data indicate that TcdA/TcdB intoxication of
403 undifferentiated and differentiated Caco-2 cells increases *C. difficile* spore adherence.
404
405 **Intoxication of IECs increases *C. difficile* spore association with E-cadherin.** Since we
406 observed that TcdA/TcdB-intoxicated differentiated Caco-2 cells lead to an increase of accessible
407 E-cadherin and adherence of *C. difficile* spores, we tested whether this could be attributed to *C.*
408 *difficile* spores associating with accessible E-cadherin. For this, unintoxicated or TcdA/TcdB-
409 intoxicated differentiated Caco-2 cells were infected with *C. difficile* spores for 1 h. Then,
410 accessible E-cadherin and spores were immunostained and visualized by confocal microscopy
411 (Figure 4*A*, *D*). Plot profile analysis of unintoxicated Caco-2 cells (Figure 4*A*) reveals that ~21%
412 of adhered *C. difficile* spores were associated with accessible E-cadherin (Figure 4*B, C,* and *G*).
413 Notably, upon TcdA/TcdB-intoxication (Figure 4*D*), ~72% of adhered spores were associated with
414 accessible E-cadherin (Figure 4*E*, *F, G*). These results indicate that adhered *C. difficile* spores can
415 associate with accessible E-cadherin in IECs, and this association is enhanced upon TcdA/TcdB-
416 intoxication.
417

418 **Antibody blocking of accessible E-cadherin reduces adherence and internalization of *C.***
419 ***difficile* spores to IECs.** Next, we assessed whether E-cadherin is involved in *C. difficile* spore
420 adherence and internalization. We have shown that *C. difficile* spore internalization occurs in the
421 presence of serum (20). Therefore, undifferentiated, differentiated, and polarized Caco-2 cells
422 were incubated with anti-E-cadherin antibody for 2h and subsequently infected for 3h with FBS-
423 incubated *C. difficile* spores. To identify intracellular spores, we used the intracellular spore
424 exclusion immunostaining assay (20), where only extracellular spores are immunostained in non-
425 permeabilized cells, and total spores are visualized by phase-contrast microscopy. Using this
426 strategy in undifferentiated Caco-2 cells, we observed that *C. difficile* spore adherence to IECs was
427 significantly decreased upon increasing concentrations of anti-E-cadherin antibody; spore
428 adherence decreased by 38, 53, and 73% compared to the control when cells were incubated with
429 1, 10, and 100 μg mL^{-1} of anti-E-cadherin antibody, respectively (Figure 5*A*). Upon quantifying
430 internalization in undifferentiated Caco-2 cells, we observed a significant decrease of 38, 43, and
431 69% compared to the control in cells incubated with 1, 10, 100 μg mL^{-1} of anti-E-cadherin,
432 respectively (Figure 5*B*). Similarly, in differentiated Caco-2 cells, a significant decrease in spore
433 adherence in 18, 32, 60, and 70% compared to the control was observed in cells incubated with
434 0.1, 1, 10, and 100 μg mL^{-1} of anti-E-cadherin, respectively (Figure 5*C*). For internalization, we
435 observed a significant decrease in 15, 35, 42, and 54% compared to the control in cells incubated
436 with 0.1, 1, 10, and 100 μg mL^{-1} of anti-E-cadherin, respectively (Figure 5*D*). Finally, in polarized
437 Caco-2 cells, we observed a decrease in 32, 56, 63, and 79% in spore adherence compared to the
438 control in presence with 0.1, 1, 10, and 100 μg mL^{-1} of anti-E-cadherin, respectively (Figure 5*E*).
439 These data indicate that the antibody-mediated blockage of accessible E-cadherin reduces *C.*
440 *difficile* spore adherence and internalization to IECs.

441

442 **Purified recombinant human E-cadherin competitively inhibits spore adherence in**
443 **undifferentiated, differentiated and TcdA/TcdB intoxicated IECs cells.** Subsequently, to
444 provide further evidence that E-cadherin acts as a spore adherence receptors, we evaluated whether
445 infected healthy undifferentiated Caco-2 monolayers with *C. difficile* spores preincubated with 1,
446 2.5, 5, 10, and 25 µg mL^{-1} of E-cadherin, and we observed a decrease in spore adherence of 12%,
447 26%, 38%, 47% and 64% respectively compared to spores not incubated with E-cadherin (Fig.
448 6*E*). In differentiated Caco-2 cells, we observed a decrease in spore adherence of 27%, 30%, 30%,
449 27% and 53% for spores incubated with 1, 2.5, 5, 10, and 25 µg mL^{-1} of E-cadherin, respectively
450 (Figure. 6*F*). Finally, we also assessed whether the increased spore adherence that we previously
451 observe in TcdA/TcdB intoxicated Caco-2 cells was E-cadherin specific. As expected, significant
452 *C. difficile* spore adherence to TcdA/TcdB intoxicated Caco-2 cells was observed in the absence
453 of E-cadherin; however, upon of TcdA/TcdB intoxicated differentiated and undifferentiated Caco-
454 2 cells with spores previously incubated with 25µg mL^{-1} of E-cadherin for 1 h at 37°C, and we
455 observed a significant decrease of 41% in undifferentiated (Figure 6*G*) and 55% in differentiated
456 Caco-2 cells (Figure 6*H*) compared to TcdA/TcdB intoxicated cells. Overall, these results show
457 that E-cadherin interacts with *C. difficile* spores in a dose-dependent manner and that E-cadherin-
458 ligand binding sites are non-homogeneously distributed on the *C. difficile* spore surface. There
459 results indicate that competition experiments with purified E-cadherin reduces the *C. difficile* spore
460 adherence in healthy and intoxicated cells.

461

462 **E-cadherin binds in a concentration-dependent manner to *C. difficile* spores.** To provide
463 evidence that *C. difficile* spores interact with E-cadherin, we used ELISA with *C. difficile* spore-

464 coated wells incubated with increasing concentrations of E-cadherin, or BSA as a control. E-
465 cadherin binding activity was evident in *C. difficile* spore-coated wells (Figure. 7*A*). The
466 specificity of this interaction was demonstrated by the dose-dependent binding. Additionally, we
467 evaluated the distribution of binding of E-cadherin to the spore surface by immunofluorescence.
468 Upon micrograph analysis, we observed that anti-E-cadherin immunostained spores exhibited a
469 non-homogeneous Fl. Int surrounding the spore (Figure. 7*B*). In spores, the Fl. Int. for E-cadherin
470 was 156, 189, 258, 304, and 369% relative to the control upon incubation with 1, 2.5, 5, 10, and
471 25 μg mL^{-1} of E-cadherin (Figure. 7*C*). Next, we established a Fl. Int cut-off limit for those *C.*
472 *difficile* spores that were visually associated with 2.5 μg mL^{-1} E-cadherin. Based on this threshold,
473 59, 65, and 66% of the spores were positive for E-cadherin in the presence of 5, 10, and 25 μg
474 mL^{-1} E-cadherin, respectively. Finally, we evaluated E-cadherin Fl. Int distribution for positive
475 immunodetected spores, and we observed that they were mainly distributed between 1.4-2.1
476 normalized Fl. Int. arbitrary units (Figure. 7*D*). Taken together, these results indicate that E-
477 cadherin binds in a concentration dependent manner to *C. difficile* spores, in a heterogeneous and
478 skewed manner to *C. difficile* spores.
479
480 **E-cadherin interacts with hair-like projections of *C. difficile* spores.** The outermost structure
481 of *C. difficile* spores are the hair-like projections, formed in part by BclA3, that are common in
482 epidemically relevant strains (16, 20, 42). Isogenic sporulating cultures of *C. difficile* lead to the
483 formation of spores with two exosporium morphotypes that exhibit hair-like projections, spores
484 with a thick exosporium layer display distinctive electron-dense bumps, and spores with a thin
485 exosporium lack these bumps (34, 42-44), suggesting that this exosporium morphotype diversity
486 might be contributing to E-cadherin spore-binding variability. Consequently, to gain ultrastructural

487 insight of the spore-E-cadherin interaction, *C. difficile* spores incubated with E-cadherin were
488 imaged by TEM and immunogold-labeling of E-cadherin. We observed E-cadherin-gold particles
489 in close contact with the exosporium of *C. difficile* spores, particularly with the hair-like
490 projections (Figure 8*A*-*E*). No gold particles were observed in spores without the E-cadherin
491 incubation. (Figure 8*A*). Next, within the E-cadherin positive spores, we observed gold particles
492 in 52/236 (22.1%) of the spores (Figure 8*F*). Of these, 19/52 (36.5%) and 33/52 (63.5%) of the E-
493 cadherin-bound spores corresponded to spores with thin and thick exosporiums, respectively
494 (Figure 8*G*). These results are representative of a 90 nm-slice of the sample, and therefore the
495 number of gold particles corresponds to those only present in the slice and not of a complete spore.
496 These results suggest that E-cadherin binds preferentially to thick-exosporium layer spores, which
497 seem to have enriched in hair-like projections.
498 and specifically to the hair-like projections.
499 Most *C. difficile* genomes encode three *bclA* orthologues encodes three collagen-like
500 proteins of the BclA family of proteins (45). However, *C. difficile* strain R20291 only encodes two
501 *bclA* orthologues (i.e., *bclA2* and *bclA3*) (45). Therefore, we reasoned to use previously
502 characterized *bclA1*, *bclA2* and *bclA3* mutants in strain 630 (30) to address by ELISA whether
503 these collagen-like proteins could be implicated in E-cadherin binding to *C. difficile* spores. As
504 with R20291 spores, E-cadherin binding to 630 spore coated wells was evident (Figure 8E).
505 Notably, upon coating wells with spores of *bclA1*, *bclA2* or *bclA3* spores, a dose dependent binding
506 of E-cadherin to spore-coated wells that as similar to that of wild-type spores, with the exception
507 of *bclA3* spores which exhibited higher binding of E-cadherin (Figure 8E). Overall, these results
508 suggest the presence of an unidentified E-cadherin-specific spore surface ligand.
509

510 **DISCUSSION**

511 A major clinical challenge that remains unresolved is how to address the high rates of CDI
512 recurrence (46-48). *C. difficile* spores are regarded as the key virulence factors required for
513 recurrence and transmission of the disease (16, 17). Although significant work has advanced our
514 understanding of the biology of *C. difficile* spores (16, 42), the mechanisms through which *C.*
515 *difficile* spores interact with the host within the environment of the colon remain poorly described.
516 The integrity of the intestinal epithelial barrier is key in preventing pathogen translocation (22).
517 However, in the healthy intestinal mucosa, the apical- and basolateral-cell sides are not always
518 separated. The adherens junctions, where E-cadherin is located, can be accessible in certain
519 situations, i.e., along lateral membranes of goblet cells (20, 49, 50), extruding apoptotic sites,
520 produced transiently when senescent cells are expelled and detached from the epithelium (49, 51,
521 52) and in epithelial folds of the intestinal villus produced by tension and constriction forces (49).
522 In this context, we have demonstrated that E-cadherin is a novel spore adherence-receptor that
523 promotes binding of *C. difficile* spores at adherens junctions, and this binding is enhanced in
524 intoxicated IECs.

525 Work by others have demonstrated that E-cadherin is hijacked by several pathogens,
526 including *Listeria monocytogenes*, *Fusobacterium nucleatum*, and *Streptococcus pneumoniae* (23-
527 26, 49). This report expands the list of pathogens that hijack E-cadherin for adherence and entry
528 to include *C. difficile* spores. Our prior work had demonstrated that *C. difficile* spores adhere to
529 IECs *in vitro* (18) and gain entry into host cells via fibronectin and vitronectin in an integrin-
530 dependent pathway (20). The ~70-80% reduction in adherence in undifferentiated, differentiated
531 and polarized monolayers of Caco-2 cells upon blockade with anti-E-cadherin antibodies or
532 competition with purified E-cadherin, suggests that E-cadherin is a major cellular adherence

533 receptor for *C. difficile* spores. Fibronectin, vitronectin, and integrin receptors are typically located
534 in the basolateral membrane (41, 53-56), where E-cadherin is localized. An outstanding question
535 is whether E-cadherin acts as an anchoring protein allowing *C. difficile* spores to bind
536 fibronectin/vitronectin and their cognate integrins to trigger internalization, or whether spore-
537 binding to E-cadherin alone is capable of triggering a signal for internalization of *C. difficile*
538 spores. This question will be addressed in future studies.
539
540 Another conclusion of this work is that *C. difficile* spores bind to E-cadherin in a dose-
541 dependent manner. *L. monocytogenes* interacts with human and not with mouse E-cadherin
542 through InlA (26). While the exosporium of *C. difficile* spores has no orthologs of InlA (57), we
543 show E-cadherin binding to the hair-like projections of the exosporium. *C. difficile* spores form
544 two exosporium morphotypes during sporulation (i.e., a thick and a thin exosporium layer) (42);
545 among the main differences is the presence of electron-dense bumps underlying the hair-like
546 projections. Whether there are differences in the hair-like projections and in their numbers between
547 both morphotypes, is unclear, and matter of study in our laboratory. The relevance of the
548 exosporium thickness in E-cadherin binding. Notably, spores of *bclA1* and *bclA2* orthologue in
549 strain 630 were able to bind to E-cadherin to a similar extent as wild-type spores, suggesting either
550 redundance in function. It was surprising to observe that *bclA3* mutant spores bind higher levels
551 of E-cadherin, suggesting that absence of BclA3 might uncover an alternative spore surface
552 ligand(s) implicated in binding of E-cadherin to the spore surface. Current ongoing work in our
553 laboratory aims to identify the spore surface ligand(s) that bind to E-cadherin and its implication
554 in disease.
555

556 A final and major conclusion of this work is that TcdA/TcdB intoxication increases spore
557 adherence to IECs in a E-cadherin-specific manner. This is supported by increased association
558 between basolateral E-cadherin and *C. difficile* spores, and by the observation that soluble E-
559 cadherin can reduce the adherence of *C. difficile* spores to TcdA/TcdB intoxicated IECs. *C. difficile*
560 toxins TcdA and TcdB cause a disruption of the cell-cell junctions (10, 12, 13), causing a loss of
561 cellular polarity (9-11). This disruption is caused by a dissociation of tight and adherens junction
562 proteins. In this context, our work contributes to understanding how *C. difficile* spores interact
563 with TcdA/TcdB-intoxicated IECs. Our results demonstrate that differentiated TcdA/TcdB-
564 intoxicated monolayers show an increased accessibility of E-cadherin that correlates with an
565 increase in spore adherence to TcdA/TcdB-intoxicated cells. These observations suggest that
566 during CDI, TcdA and TcdB increase the E-cadherin accessibility, contributing to the spore
567 adherence and entry into the IECs *in vivo*. Indeed, since intracellular *C. difficile* spores contribute
568 to disease recurrence (20), TcdA/TcdB -intoxication may significantly contribute to *C. difficile*
569 spore adherence and internalization during CDI, contributing overall to disease recurrence. These
570 hypotheses are in agreement with clinical observations in CDI patients where high titers of
571 endogenous antibodies against the *C. difficile* toxins correlate with reduced R-CDI rates (58), and
572 with the reduced R-CDI observed in the clinical trials of bezlotoxumab (15). The development of
573 multifactorial treatment with intervention in TcdA/TcdB, spore adherence, and entry to IECs might
574 importantly reduce the R-CDI rates.
575

576 **NOTES**

577 ***CONFLICT OF INTEREST***. The authors declare that they have no conflict of interest.

578

579 ***FUNDING.*** This work was funded by FONDECYT Regular 1191601, and by Millennium Science

580 Initiative Program – NCN17_093, and Startup funds from the Department of Biology at Texas

581 A&M University to D.P-S. Additional funding support to P.C-C from ANID-PCHA/Doctorado

582 Nacional/ 2016-21161395.

583

584 **REFERENCES**

585

586 1. Redelings MD, Sorvillo F, Mascola L. 2007. Increase in *Clostridium difficile*-related
587 mortality rates, United States, 1999-2004. Emerg Infect Dis 13:1417-9.
588 2. Stevens VW, Nelson RE, Schwab-Daugherty EM, Khader K, Jones MM, Brown KA, Greene
589 T, Croft LD, Neuhauser M, Glassman P, Goetz MB, Samore MH, Rubin MA. 2017.
590 Comparative Effectiveness of Vancomycin and Metronidazole for the Prevention of
591 Recurrence and Death in Patients With *Clostridium difficile* Infection. JAMA Intern Med
592 177:546-553.
593 3. Di X, Bai N, Zhang X, Liu B, Ni W, Wang J, Wang K, Liang B, Liu Y, Wang R. 2015. A meta-
594 analysis of metronidazole and vancomycin for the treatment of *Clostridium difficile*
595 infection, stratified by disease severity. Braz J Infect Dis 19:339-49.
596 4. Lyerly DM, Lockwood DE, Richardson SH, Wilkins TD. 1982. Biological activities of toxins
597 A and B of *Clostridium difficile*. Infect Immun 35:1147-50.
598 5. Lyras D, O'Connor JR, Howarth PM, Sambol SP, Carter GP, Phumoonna T, Poon R, Adams
599 V, Vedantam G, Johnson S, Gerding DN, Rood JI. 2009. Toxin B is essential for virulence of
600 *Clostridium difficile*. Nature 458:1176-9.
601 6. Kuehne SA, Cartman ST, Heap JT, Kelly ML, Cockayne A, Minton NP. 2010. The role of toxin
602 A and toxin B in *Clostridium difficile* infection. Nature 467:711-3.
603 7. Just I, Selzer J, Wilm M, von Eichel-Streiber C, Mann M, Aktories K. 1995. Glucosylation of
604 Rho proteins by *Clostridium difficile* toxin B. Nature 375:500-3.
605 8. Just I, Wilm M, Selzer J, Rex G, von Eichel-Streiber C, Mann M, Aktories K. 1995. The
606 enterotoxin from *Clostridium difficile* (ToxA) monoglucosylates the Rho proteins. J Biol
607 Chem 270:13932-6.
608 9. Nusrat A, von Eichel-Streiber C, Turner JR, Verkade P, Madara JL, Parkos CA. 2001.
609 *Clostridium difficile* toxins disrupt epithelial barrier function by altering membrane
610 microdomain localization of tight junction proteins. Infect Immun 69:1329-36.
611 10. Mileto SJ, Jardé T, Childress KO, Jensen JL, Rogers AP, Kerr G, Hutton ML, Sheedlo MJ,
612 Bloch SC, Shupe JA, Horvay K, Flores T, Engel R, Wilkins S, McMurrick PJ, Lacy DB, Abud
613 HE, Lyras D. 2020. *Clostridioides difficile* infection damages colonic stem cells via TcdB,
614 impairing epithelial repair and recovery from disease. Proc Natl Acad Sci U S A 117:8064-
615 8073.
616 11. Kasendra M, Barrile R, Leuzzi R, Soriani M. 2014. *Clostridium difficile* toxins facilitate
617 bacterial colonization by modulating the fence and gate function of colonic epithelium. J
618 Infect Dis 209:1095-104.
619 12. Hecht G, Pothoulakis C, LaMont JT, Madara JL. 1988. *Clostridium difficile* toxin A perturbs
620 cytoskeletal structure and tight junction permeability of cultured human intestinal
621 epithelial monolayers. J Clin Invest 82:1516-24.
622 13. Hecht G, Koutsouris A, Pothoulakis C, LaMont JT, Madara JL. 1992. *Clostridium difficile*
623 toxin B disrupts the barrier function of T84 monolayers. Gastroenterology 102:416-23.

624 14. Leslie JL, Huang S, Opp JS, Nagy MS, Kobayashi M, Young VB, Spence JR. 2015. Persistence
625 and toxin production by *Clostridium difficile* within human intestinal organoids result in
626 disruption of epithelial paracellular barrier function. Infect Immun 83:138-45.
627 15. Wilcox MH, Gerding DN, Poxton IR, Kelly C, Nathan R, Birch T, Cornely OA, Rahav G, Bouza
628 E, Lee C, Jenkin G, Jensen W, Kim YS, Yoshida J, Gabryelski L, Pedley A, Eves K, Tipping R,
629 Guris D, Kartsonis N, Dorr MB, Investigators MIaMI. 2017. Bezlotoxumab for Prevention
630 of Recurrent *Clostridium difficile* Infection. N Engl J Med 376:305-317.
631 16. Paredes-Sabja D, Shen A, Sorg JA. 2014. *Clostridium difficile* spore biology: sporulation,
632 germination, and spore structural proteins. Trends Microbiol 22:406-16.
633 17. Deakin LJ, Clare S, Fagan RP, Dawson LF, Pickard DJ, West MR, Wren BW, Fairweather NF,
634 Dougan G, Lawley TD. 2012. The *Clostridium difficile spo0A* gene is a persistence and
635 transmission factor. Infect Immun 80:2704-11.
636 18. Paredes-Sabja D, Sarker MR. 2012. Adherence of *Clostridium difficile* spores to Caco-2
637 cells in culture. J Med Microbiol 61:1208-1218.
638 19. Mora-Uribe P, Miranda-Cardenas C, Castro-Cordova P, Gil F, Calderon I, Fuentes JA, Rodas
639 PI, Banawas S, Sarker MR, Paredes-Sabja D. 2016. Characterization of the Adherence of
640 *Clostridium difficile* Spores: The Integrity of the Outermost Layer Affects Adherence
641 Properties of Spores of the Epidemic Strain R20291 to Components of the Intestinal
642 Mucosa. Front Cell Infect Microbiol 6:99.
643 20. Castro-Córdova P, Mora-Uribe P, Reyes-Ramírez R, Cofré-Araneda G, Orozco-Aguilar J,
644 Brito-Silva C, Mendoza-León MJ, Kuehne SA, Minton NP, Pizarro-Guajardo M, Paredes-
645 Sabja D. 2021. Entry of spores into intestinal epithelial cells contributes to recurrence of
646 *Clostridioides difficile* infection. Nat Commun 12:1140.
647 21. Buckley A, Turner JR. 2018. Cell Biology of Tight Junction Barrier Regulation and Mucosal
648 Disease. Cold Spring Harb Perspect Biol 10.
649 22. Paradis T, Bègue H, Basmaciyan L, Dalle F, Bon F. 2021. Tight Junctions as a Key for
650 Pathogens Invasion in Intestinal Epithelial Cells. Int J Mol Sci 22.
651 23. Rubinstein MR, Wang X, Liu W, Hao Y, Cai G, Han YW. 2013. *Fusobacterium nucleatum*
652 promotes colorectal carcinogenesis by modulating E-cadherin/β-catenin signaling via its
653 FadA adhesin. Cell Host Microbe 14:195-206.
654 24. Anderton JM, Rajam G, Romero-Steiner S, Summer S, Kowalczyk AP, Carlone GM,
655 Sampson JS, Ades EW. 2007. E-cadherin is a receptor for the common protein
656 pneumococcal surface adhesin A (PsaA) of *Streptococcus pneumoniae*. Microb Pathog
657 42:225-36.
658 25. Elmi A, Nasher F, Jagatia H, Gundogdu O, Bajaj-Elliott M, Wren B, Dorrell N. 2016.
659 *Campylobacter jejuni* outer membrane vesicle-associated proteolytic activity promotes
660 bacterial invasion by mediating cleavage of intestinal epithelial cell E-cadherin and
661 occludin. Cell Microbiol 18:561-72.
662 26. Mengaud J, Ohayon H, Gounon P, Mege R-M, Cossart P. 1996. E-cadherin is the receptor
663 for internalin, a surface protein required for entry of *L. monocytogenes* into epithelial
664 cells. Cell 84:923-32.
665 27. Ribet D, Cossart P. 2015. How bacterial pathogens colonize their hosts and invade deeper
666 tissues. Microbes Infect 17:173-83.

667 28. Ng YK, Ehsaan M, Philip S, Collery MM, Janoir C, Collignon A, Cartman ST, Minton NP.
668 2013. Expanding the repertoire of gene tools for precise manipulation of the *Clostridium*
669 *difficile* genome: allelic exchange using *pyrE* alleles. PLoS One 8:e56051.
670 29. Wüst J, Sullivan NM, Hardegger U, Wilkins TD. 1982. Investigation of an outbreak of
671 antibiotic-associated colitis by various typing methods. J Clin Microbiol 16:1096-101.
672 30. Phetcharaburanin J, Hong HA, Colenutt C, Bianconi I, Sempere L, Permpoonpattana P,
673 Smith K, Dembek M, Tan S, Brisson MC, Brisson AR, Fairweather NF, Cutting SM. 2014.
674 The spore-associated protein BclA1 affects the susceptibility of animals to colonization
675 and infection by *Clostridium difficile*. Mol Microbiol 92:1025-38.
676 31. Chandrasekaran R, Kenworthy AK, Lacy DB. 2016. *Clostridium difficile* Toxin A Undergoes
677 Clathrin-Independent, PACSIN2-Dependent Endocytosis. PLoS Pathog 12:e1006070.
678 32. Calderon-Romero P, Castro-Cordova P, Reyes-Ramirez R, Milano-Cespedes M, Guerrero-
679 Araya E, Pizarro-Guajardo M, Olguin-Araneda V, Gil F, Paredes-Sabja D. 2018. *Clostridium*
680 *difficile* exosporium cysteine-rich proteins are essential for the morphogenesis of the
681 exosporium layer, spore resistance, and affect *C. difficile* pathogenesis. PLoS Pathog
682 14:e1007199.
683 33. Pizarro-Guajardo M, Diaz-Gonzalez F, Alvarez-Lobos M, Paredes-Sabja D. 2017.
684 Characterization of Chicken IgY Specific to *Clostridium difficile* R20291 Spores and the
685 Effect of Oral Administration in Mouse Models of Initiation and Recurrent Disease. Front
686 Cell Infect Microbiol 7:365.
687 34. Pizarro-Guajardo M, Calderon-Romero P, Castro-Cordova P, Mora-Uribe P, Paredes-Sabja
688 D. 2016. Ultrastructural Variability of the Exosporium Layer of *Clostridium difficile* Spores.
689 Appl Environ Microbiol 82:2202-2209.
690 35. Schöttelndreier D, Langejürgen A, Lindner R, Genth H. 2020. Low Density Lipoprotein
691 Receptor-Related Protein-1 (LRP1) Is Involved in the Uptake of *Clostridioides difficile* Toxin
692 A and Serves as an Internalizing Receptor. Front Cell Infect Microbiol 10:565465.
693 36. Tam J, Icho S, Utama E, Orrell KE, Gómez-Biagi RF, Theriot CM, Kroh HK, Rutherford SA,
694 Lacy DB, Melnyk RA. 2020. Intestinal bile acids directly modulate the structure and
695 function of *C.difficile* TcdB toxin. Proc Natl Acad Sci U S A 117:6792-6800.
696 37. Landenberger M, Nieland J, Roeder M, Nørgaard K, Papatheodorou P, Ernst K, Barth H.
697 2021. The cytotoxic effect of *Clostridioides difficile* pore-forming toxin CDTb. Biochim
698 Biophys Acta Biomembr 1863:183603.
699 38. Aktories K, Schwan C, Jank T. 2017. *Clostridium difficile* toxin biology. Annu Rev Microbiol
700 71:281-307.
701 39. Kroh HK, Chandrasekaran R, Zhang Z, Rosenthal K, Woods R, Jin X, Nyborg AC, Rainey GJ,
702 Warrener P, Melnyk RA, Spiller BW, Lacy DB. 2018. A neutralizing antibody that blocks
703 delivery of the enzymatic cargo of *Clostridium difficile* toxin TcdB into host cells. J Biol
704 Chem 293:941-952.
705 40. Schwan C, Stecher B, Tzivelekidis T, van Ham M, Rohde M, Hardt WD, Wehland J, Aktories
706 K. 2009. *Clostridium difficile* toxin CDT induces formation of microtubule-based
707 protrusions and increases adherence of bacteria. PLoS Pathog 5:e1000626.
708 41. Schwan C, Kruppke AS, Nolke T, Schumacher L, Koch-Nolte F, Kudryashev M, Stahlberg H,
709 Aktories K. 2014. *Clostridium difficile* toxin CDT hijacks microtubule organization and

710 reroutes vesicle traffic to increase pathogen adherence. Proc Natl Acad Sci U S A
711 111:2313-8.
712 42. Paredes-Sabja D, Cid-Rojas F, Pizarro-Guajardo M. 2022. Assembly of the exosporium
713 layer in Clostridioides difficile spores. Curr Opin Microbiol 67:102137.
714 43. Pizarro-Guajardo M, Calderon-Romero P, Paredes-Sabja D. 2016. Ultrastructure
715 Variability of the Exosporium Layer of *Clostridium difficile* Spores from Sporulating
716 Cultures and Biofilms. Appl Environ Microbiol 82:5892-8.
717 44. Pizarro-Guajardo M, Calderón-Romero P, Romero-Rodríguez A, Paredes-Sabja D. 2020.
718 Characterization of Exosporium Layer Variability of C*lostridioides difficile* Spores in the
719 Epidemically Relevant Strain R20291. Front Microbiol 11:1345.
720 45. Pizarro-Guajardo M, Olguin-Araneda V, Barra-Carrasco J, Brito-Silva C, Sarker MR,
721 Paredes-Sabja D. 2014. Characterization of the collagen-like exosporium protein, BclA1,
722 of *Clostridium difficile* spores. Anaerobe 25:18-30.
723 46. Lessa FC, Mu Y, Bamberg WM, Beldavs ZG, Dumyati GK, Dunn JR, Farley MM, Holzbauer
724 SM, Meek JI, Phipps EC, Wilson LE, Winston LG, Cohen JA, Limbago BM, Fridkin SK, Gerding
725 DN, McDonald LC. 2015. Burden of *Clostridium difficile* infection in the United States. N
726 Engl J Med 372:825-34.
727 47. Kelly CP. 2012. Can we identify patients at high risk of recurrent *Clostridium difficile*
728 infection? Clin Microbiol Infect 18:21-7.
729 48. Zhang S, Palazuelos-Munoz S, Balsells EM, Nair H, Chit A, Kyaw MH. 2016. Cost of hospital
730 management of Clostridium difficile infection in United States-a meta-analysis and
731 modelling study. BMC Infect Dis 16:447.
732 49. Nikitas G, Deschamps C, Disson O, Niault T, Cossart P, Lecuit M. 2011. Transcytosis of
733 *Listeria monocytogenes* across the intestinal barrier upon specific targeting of goblet cell
734 accessible E-cadherin. J Exp Med 208:2263-77.
735 50. Gessain G, Tsai YH, Travier L, Bonazzi M, Grayo S, Cossart P, Charlier C, Disson O, Lecuit
736 M. 2015. PI3-kinase activation is critical for host barrier permissiveness to *Listeria*
737 *monocytogenes*. J Exp Med 212:165-83.
738 51. Pentecost M, Otto G, Theriot JA, Amieva MR. 2006. *Listeria monocytogenes* invades the
739 epithelial junctions at sites of cell extrusion. PLoS Pathog 2:e3.
740 52. Pentecost M, Kumaran J, Ghosh P, Amieva MR. 2010. *Listeria monocytogenes* internalin B
741 activates junctional endocytosis to accelerate intestinal invasion. PLoS Pathog
742 6:e1000900.
743 53. Singh B, Su YC, Riesbeck K. 2010. Vitronectin in bacterial pathogenesis: a host protein used
744 in complement escape and cellular invasion. Mol Microbiol 78:545-60.
745 54. Henderson B, Nair S, Pallas J, Williams MA. 2011. Fibronectin: a multidomain host adhesin
746 targeted by bacterial fibronectin-binding proteins. FEMS Microbiol Rev 35:147-200.
747 55. Hamzaoui N, Kernéis S, Caliot E, Pringault E. 2004. Expression and distribution of beta1
748 integrins in in vitro-induced M cells: implications for *Yersinia* adhesion to Peyer's patch
749 epithelium. Cell Microbiol 6:817-28.
750 56. Clark MA, Hirst BH, Jepson MA. 1998. M-cell surface beta1 integrin expression and
751 invasin-mediated targeting of *Yersinia pseudotuberculosis* to mouse Peyer's patch M cells.
752 Infect Immun 66:1237-43.

753 57. Diaz-Gonzalez F, Milano M, Olguin-Araneda V, Pizarro-Cerda J, Castro-Cordova P, Tzeng
754 SC, Maier CS, Sarker MR, Paredes-Sabja D. 2015. Protein composition of the outermost
755 exosporium-like layer of *Clostridium difficile* 630 spores. J Proteomics 123:1-13.
756 58. Kelly CP, Poxton IR, Shen J, Wilcox MH, Gerding DN, Zhao X, Laterza OF, Railkar R, Guris
757 D, Dorr MB. 2020. Effect of Endogenous *Clostridioides difficile* Toxin Antibodies on
758 Recurrence of *C. difficile* Infection. Clin Infect Dis 71:81-86.
759

760

761

762

763 **Figure Legends**

764 **Figure 1. Distribution of accessible and total E-cadherin in undifferentiated and**
765 **differentiated Caco-2 cells.** 3D projection of a representative confocal micrograph of healthy *A*,
766 undifferentiated, and *B*, differentiated Caco-2 cells immunostaining for accessible E-cadherin.
767 Accessible E-cadherin (shown as acc Ecad) is in green, F-actin in red, and nuclei in blue. *C*,
768 Repartition of cells that were positive (Ecad+) or negative (Ecad−) stained for accessible E-
769 cadherin. 3D projection of a representative confocal micrograph of a healthy *D*, undifferentiated
770 and *E*, differentiated Caco-2 cells immunostaining for total E-cadherin and *F*, Repartition of cells
771 that were positive (Ecad+) or negative (Ecad−) stained for total E-cadherin. Fluorophores colors
772 were digitally reassigned for a better representation. Micrographs are representative of 6 fields of
773 2 independent experiments. Scale bar, 20µm. Error bars indicate mean ± SEM. Statistical analysis
774 was performed by two-tailed unpaired Student's *t*-test, ns, $p > 0.05$; ****, $p \leq 0.0001$.

775

776 **Figure 2. The accessibility of E-cadherin increases in TcdA and TcdB intoxicated IECs.**
777 Differentiated TcdA/TcdB intoxicated Caco-2 cells for 3, 6, or 8 h in DMEM without serum. As a
778 control, cells were incubated with DMEM without serum. Non-permeabilized cells were stained
779 for accessible E-cadherin (shown as acc Ecad; green), permeabilized, and total E-cadherin was
780 stained (shown as total Ecad; red) and nuclei (blue). *A*, Representative confocal microscopy images
781 3D (XY) projection of control cells (left) and TcdA/TcdB intoxicated cells for 8h (right); below
782 the orthogonal view (XZ; accessible E-cadherin, total E-cadherin and merged) of the dotted line
783 of the XY. Representative confocal images for 3h and 8h not shown. Relative Fl. Int. measured as
784 the sum of each z-step of *B*, accessible E-cadherin, and its abundance in the *C*, apical side, or *D* in
785 the basal side of the cell. Relative Fl.Int. of *E*, total E-cadherin, its abundance in the *F*, apical side,

786 and the *G*, basal side of the cell. Controls were set 100%. Error bars indicate the mean ± SEM
787 from at least 9 fields ($n = 3$). *H*, immunoblotting anti non-glucosylated Rac1 and total Rac1 of cell
788 lysates of undifferentiated and differentiated Caco-2 cells intoxicated with TcdA/TcdB for 3, 6 or
789 8h. For undifferentiated in non-glucosylated Rac1 was evaluated, then stripped and membranes
790 were tested for total Rac1. Meanwhile for differentiated cells, the same sample was solved in 2
791 independent membranes simultaneously and were independently tested for non-glucosylated and
792 total Rac1. Western blot are representative of 3 independent experiment. Statistical analysis was
793 performed by two-tailed unpaired Student's *t*-test, ns, $p > 0.05$; ****, $p < 0.0001$. Bars, 5μm.
794

795 **Figure 3. TcdA and TcdB increase *C. difficile* spore interaction with IECs.**

796 Differentiated TcdA/TcdB intoxicated Caco-2 cells for 8h or incubated with DMEM without
797 serum as control and then, were washed with PBS and infected for 3h at an MOI 10 with *C. difficile*
798 spores. Unbound spores were rinsed off. Non-permeabilized cells were stained for adhered spores.
799 *A*, Representative epifluorescence microscopy images of TcdA and TcdB intoxicated cells (or
800 DMEM as control) for 8h then washed and infected with *C. difficile* spore. *B*, *C. difficile* spore
801 adherence relative in *B*, undifferentiated and *C*, differentiated cells. In bars, each dot represents
802 one independent well from 2 independent experiment, Per well, a total of 5 fields were analyzed.
803 Error bars indicate the mean ± SEM.. Statistical analysis was performed by unpaired *t*-test, ns, $p >$
804 0.05. Bars, 10 μm.
805

806 **Figure 4. E-cadherin of IECs interacts with *C. difficile* spores increasing in TcdA and TcdB**
807 **intoxicated cells.**

808 Differentiated Caco-2 cells were intoxicated with TcdA and TcdB for 8 h at 37 °C in DMEM

809 without serum. As a control, cells were incubated with DMEM without serum. Then cells were
810 infected with *C. difficile* spores for 1 h at 37 °C. Non-permeabilized cells were stained for
811 accessible E-cadherin (shown as acc Ecad; green), spores (red), and nuclei (blue). *A*,
812 Representative 3D projection confocal micrograph of healthy cells infected with *C. difficile* spores
813 (Ctrl). On the right, magnifications of representative *C. difficile* spores associated or not with E-
814 cadherin. *B*, *C,* Plot profile Fl.Int. of *C. difficile* spores (red line) and accessible E-cadherin (shown
815 as Ecad, green line) performed in the white line of *A*. *D*, Representative 3D projection confocal
816 micrograph of TcdA and TcdB intoxicated cells infected with *C. difficile* spores. On the right
817 magnifications of representative *C. difficile* spores associated or not with E-cadherin. *E, F*, Plot
818 profile Fl.Int. of *C. difficile* spores (red) and accessible E-cadherin (shown as Ecad, in green)
819 performed in the white line of *D*. Repartition of spores that were positive (Ecad+) or negative
820 (Ecad−) associated with fluorescence signal for accessible E-cadherin was shown as the average
821 associated/non-associated spores with E-cadherin for each field, a total of ~500 spores were
822 analyzed. Fluorophores were digitally reassigned for a better representation. Micrographs are
823 representative of 6 independent fields of 3 different experiments. Error bars indicate mean ± SEM.
824 Statistical analysis was performed by two-tailed unpaired Student's *t*-test, ns, $p > 0.05$; **, $p \leq$
825 0.01; ***, $p \leq 0.001$. Bars, 10μm.
826
827 **Figure 5. E-cadherin blocking antibodies decrease the spore interaction with IECs.**
828 Undifferentiated, differentiated, and polarized Caco-2 cells were infected with *C. difficile* spores
829 preincubated with FBS in the presence of anti-E-cadherin or non-immune IgG as control for 2 h at
830 37 °C. *A*, adherence, and *B*, internalization of *C. difficile* spores in undifferentiated Caco-2 cells
831 or *C*, adherence and *D*, internalization in differentiated Caco-2. *E, C. difficile* spore adherence in

832 polarized Caco-2 cells. Data showed in each panel are normalized to 0 µg mL^{-1} of antibody.
833 The data are the mean of 6 independent wells collected in 2 independent experiments. In bars, each
834 dot represents one independent well collected from 2 independent experiments. For each bar, a
835 total of ~1,300 spores were analyzed. Error bars indicate mean ± SEM. Statistical analysis was
836 performed by two-tailed unpaired Student's *t*-test, ns, $p > 0.05$; ****, $p < 0.0001$.
837
838 **Figure 6. E-cadherin competitively reduces spore adherence to healthy and intoxicated**
839 **IECs.**
840 *A* Undifferentiated and differentiated Caco-2 cells where infected for 3 h at a MOI of 10 with *C.*
841 *difficile* spores pretreated with 1, 2.5, 5, 10 and 25µg/mL of human purified E-cadherin, and
842 adhered cells where identified and quantified as described in the Method section. *B*. TcdA/TcdB
843 intoxicated undifferentiated and differentiated Caco-2 cells where infected for 3 h at a MOI of 10
844 with *C. difficile* spores pretreated with 25µg/mL of human purified E-cadherin, and adhered cells
845 where identified and quantified as described in the Method section. The data are the mean of 6
846 independent wells collected in 2 independent experiments. Adherence of *C. difficile* spores
847 preincubated with E-cadherin (or DMEM as control) in 8 h-TcdA/TcdB intoxicated cells. The
848 data are the mean of 6 independent wells collected in 2 independent experiments.
849
850 **Figure 7. E-cadherin interacts with *C. difficile* spore.**
851 *A*, Solid-phase binding assay of *C. difficile* R20291 spores or BSA as control with increasing
852 concentrations (i.e., 0.2, 2.0, 20 and 200 nM) of human purified E-cadherin. The data represented
853 are the mean of 9 independent wells collected in 3 independent experiments. *B*, Representative
854 phase-contrast micrograph, immunofluorescence against E-cadherin, and immunofluorescence

855 plot profile of 4×10^7 *C. difficile* spores that were incubated with increasing concentrations (i.e.,
856 1, 2.5, 5, 10, 25 μg mL^{-1}) of human purified E-cadherin for 1 h at 37 °C. *C*, Quantitative analysis
857 of Fl.Int. *D*, Distribution of E-cadherin fluorescence intensity of *C. difficile* incubated with
858 increasing concentrations (i.e., 1, 2.5, 5, 10, 25 μg mL^{-1}) of human purified E-cadherin. A total of
859 ~450 spores were analyzed for each condition. Error bars indicate mean ± SEM. Statistical analysis
860 was performed by two-tailed unpaired Student's *t*-test, ns, $p > 0.05$; *, $p < 0.05$; ****, $p < 0.0001$.
861

862 **Figure 8. Immunoelectron microscopy of E-cadherin-gold complex binds to *C. difficile***
863 **spores.**

864 *A*,*B* TEM of *C. difficile* spores incubated with 10 μg mL^{-1} E-cadherin or without E-cadherin
865 (negative control). Then incubated with anti-E-cadherin and anti-mouse-gold 12 nm complex.
866 White arrows denote the mouse anti-E-cadherin and anti-mouse-gold 12 nm complex. Spores
867 where stratified in thick and thin exosporium spores. Lower panels are magnification of the black
868 squares highlighting immunogold spots, Quantification of the *C. difficile* spore associated with E-
869 cadherin ("−" and "+" denote negative or positive association, respectively). *C,D* Classification of
870 E-cadherin positively associated *C. difficile* spores according to the morphology of the spore, thin
871 or thick exosporium, represented as the percentage of the total E-cadherin positive spores. Figures
872 show representative spores with a thin or thick exosporium layer, and are representative of 2
873 independent experiments. A total of 100 spores were quantified. *E* solid-phase binding assay of
874 human E-cadherin to *C. difficile* spores of 630 wild-type and isogenic mutant strains of *bclA1*,
875 *bclA2* and *bclA3* or BSA as a control with increasing concentrations (i.e., 0.2, 2.0, 20 and 200 nM)
876 of human purified E-cadherin. The data represented are the mean of 9 independent wells collected
877 in 3 independent experiments. Statistical analysis was performed by ONE-WAY ANOVA

878 followed by Bonferroni for multicomparisons, ns, $p > 0.05$; *, $p < 0.05$, ****, $p < 0.0001$. Colors

879 correspond to the mutant strain being compared to wild-type.

880

881 **Supplementary figures review only.**

882

883 **Supplementary confocal micrographs of Fig. 1.**

884 These are supplementary figures from the experiment detailed in Fig. 4. Differentiated Caco-2
885 cells intoxicated with 600 pM of TcdA and TcdB for 3, 6, or 8 h in DMEM without serum. As a
886 control, cells were treated with DMEM without serum. Non-permeabilized cells were stained for
887 accessible E-cadherin (shown as acc Ecad) in green, then permeabilized and stained total E-
888 cadherin (total Ecad) shown in red nuclei shown in blue. Representative confocal microscopy
889 images 3D (XY) projection of intoxicated cells for 3 h (left) or 6 h (right) with its control; below
890 a magnified slide (XY), and the orthogonal view (XZ). Representative images from at 9 fields (*n*
891 = 3). Bars, 5μm.

892

893

Figure 1

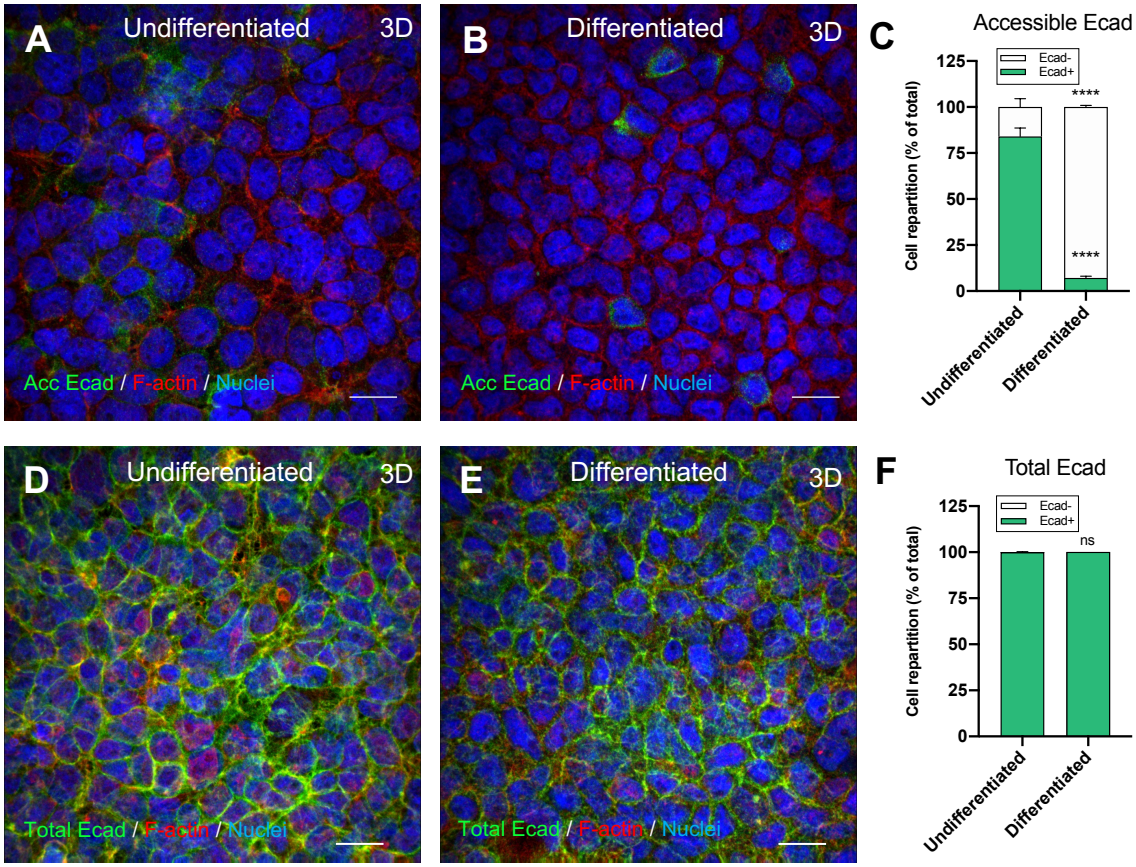
A
Undifferentiated
3D
Acc Ecad / F-actin / Nuclei
B
Differentiated
3D
Acc Ecad / F-actin / Nuclei
C
Accessible Ecad
Ecad-
Ecad+
Cell repartition (% of total)
125
100
75
50
25
0
****
****
Undifferentiated
Differentiated
D
Undifferentiated
3D
Total Ecad / F-actin / Nuclei
E
Differentiated
3D
Total Ecad / F-actin / Nuclei
F
Total Ecad
Ecad-
Ecad+
Cell repartition (% of total)
125
100
75
50
25
0
ns
Undifferentiated
Differentiated

Figure 2

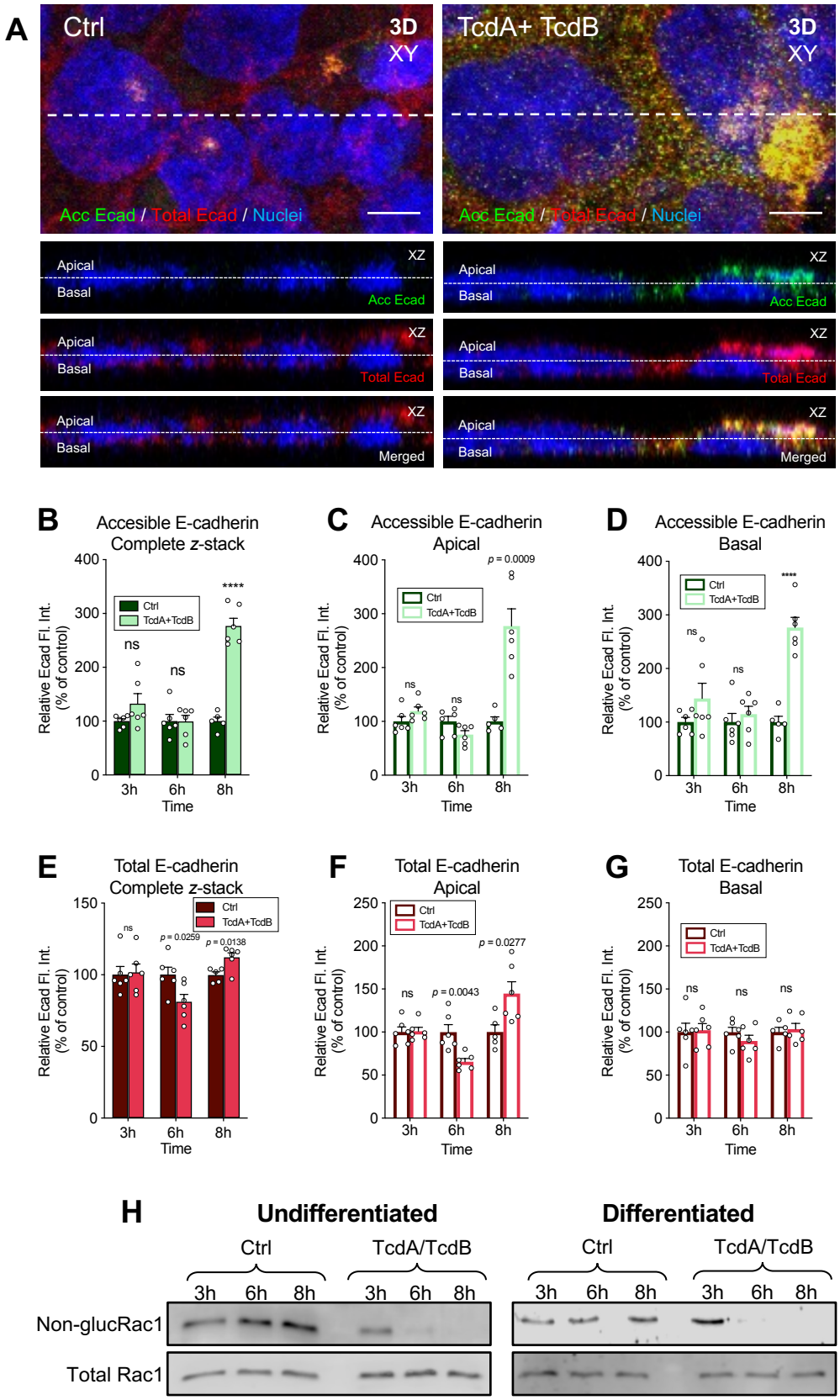
A
Ctrl
3D
XY
Acc Ecad / Total Ecad / Nuclei
TcdA+ TcdB
Apical
Basal
XZ
Acc Ecad
Total Ecad
Merged
B
Accesible E-cadherin
Complete z-stack
C
Accessible E-cadherin
Apical
D
Accessible E-cadherin
Basal
E
Total E-cadherin
Complete z-stack
F
Total E-cadherin
Apical
G
Total E-cadherin
Basal
Relative Ecad Fl. Int.
(% of control)
Ctrl
TcdA+TcdB
ns
p = 0.0009
p = 0.0259
p = 0.0138
p = 0.0043
p = 0.0277
3h
6h
8h
Time
H
Undifferentiated
Differentiated
Ctrl
TcdA/TcdB
Non-glucRac1
Total Rac1

Figure 3

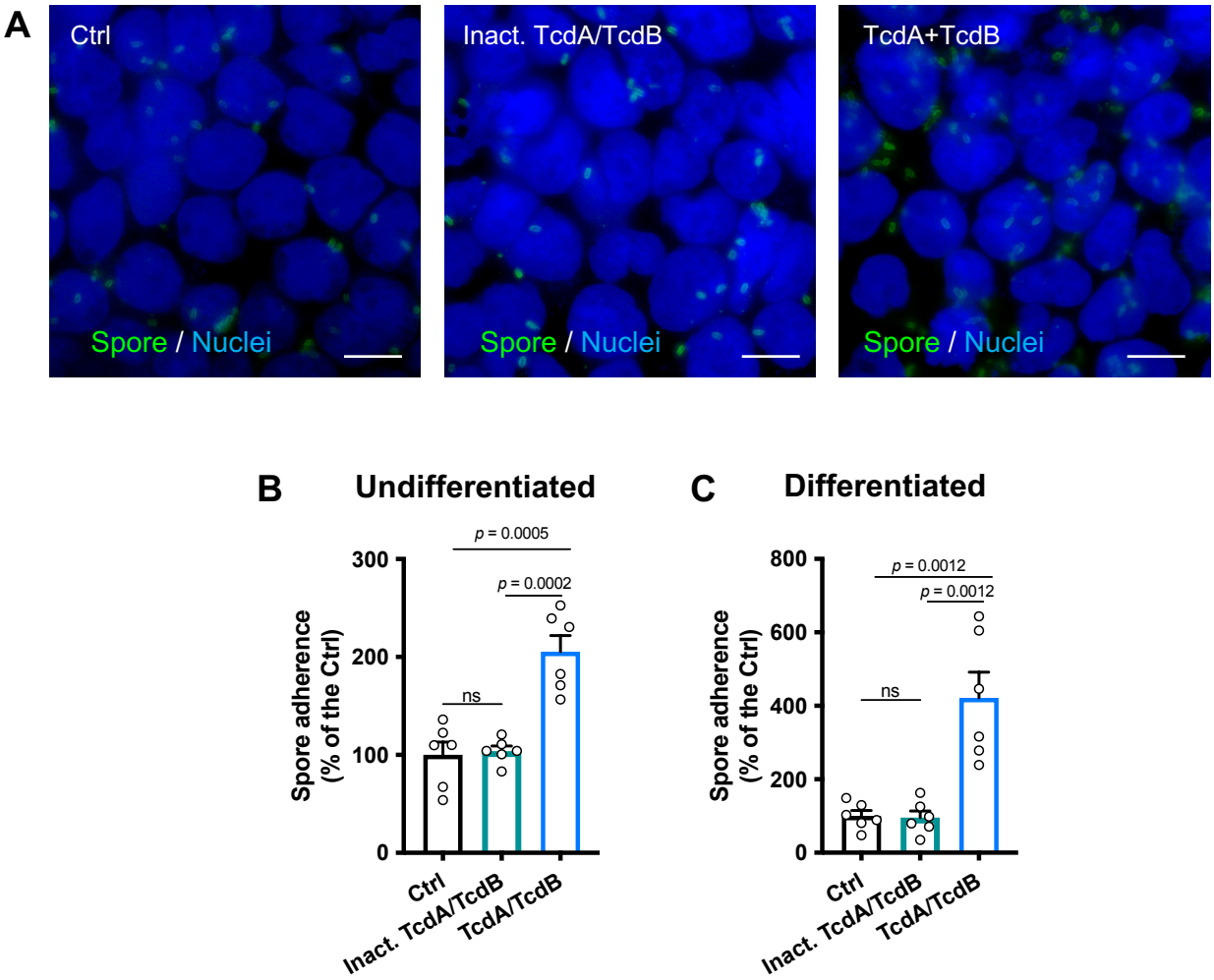
A
Ctrl
Spore / Nuclei
Inact. TcdA/TcdB
Spore / Nuclei
TcdA+TcdB
Spore / Nuclei
B
Undifferentiated
Spore adherence (% of the Ctrl)
300
200
100
0
p = 0.0005
p = 0.0002
ns
Ctrl
Inact. TcdA/TcdB
TcdA/TcdB
C
Differentiated
Spore adherence (% of the Ctrl)
800
600
400
200
0
p = 0.0012
p = 0.0012
ns
Ctrl
Inact. TcdA/TcdB
TcdA/TcdB

Figure 4

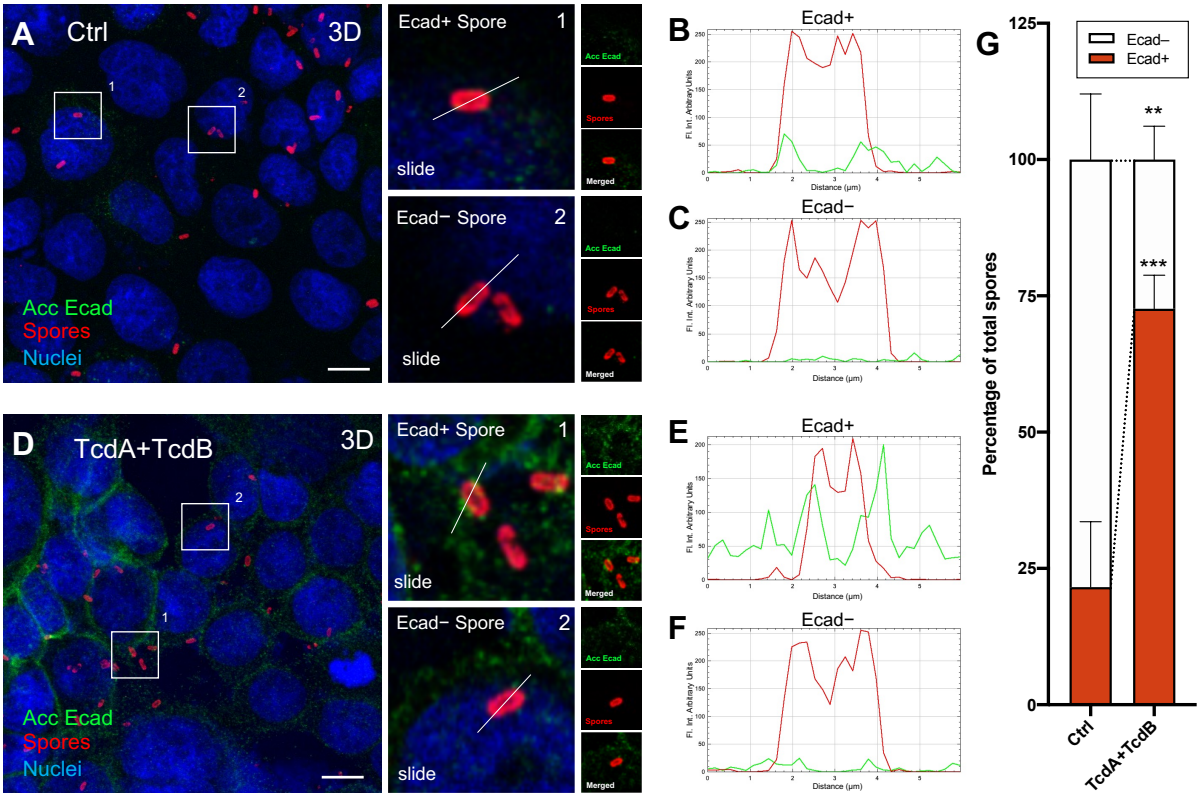
A
Ctrl
3D
1
2
Acc Ecad
Spores
Nuclei
Ecad+ Spore
1
slide
Ecad− Spore
2
slide
Acc Ecad
Spores
Merged
B
Ecad+
C
Ecad−
E
Ecad+
F
Ecad−
Fl. Int. Arbitrary Units
Distance (µm)
D
TcdA+TcdB
3D
1
2
Acc Ecad
Spores
Nuclei
Ecad+ Spore
1
slide
Ecad− Spore
2
slide
Acc Ecad
Spores
Merged
G
Ecad−
Ecad+
Percentage of total spores
125
100
75
50
25
0
**
***
Ctrl
TcdA+TcdB

Figure 5

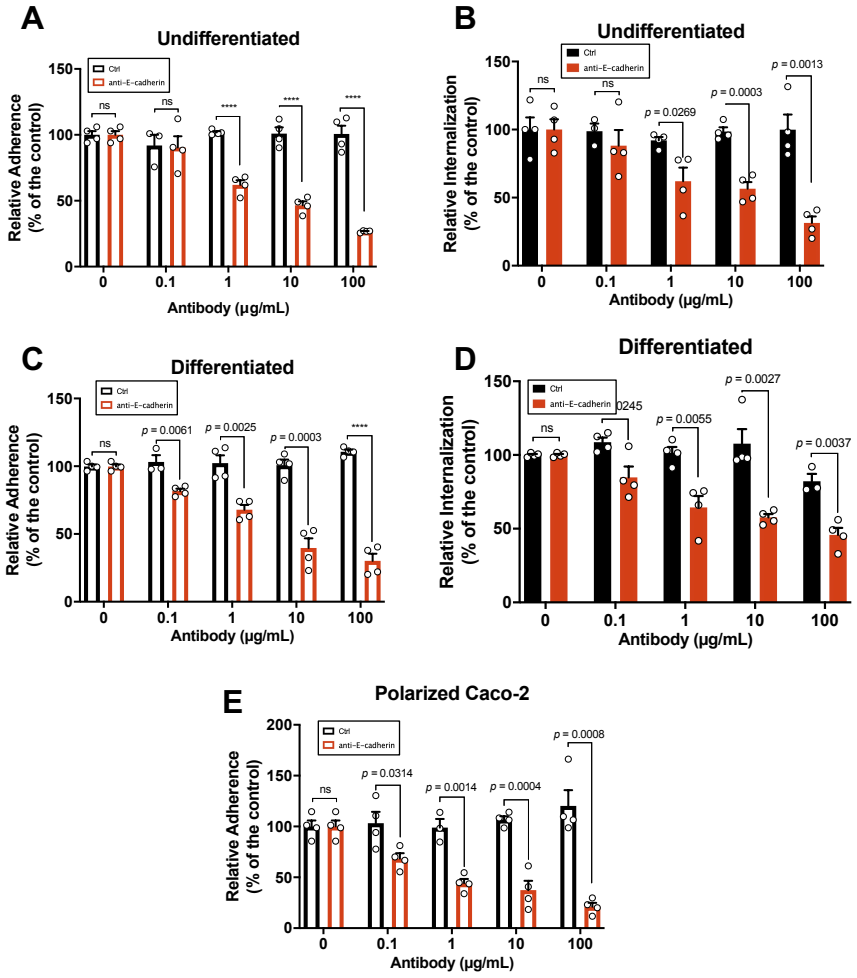
A
Undifferentiated
Ctrl
anti-E-cadherin
Relative Adherence (% of the control)
ns
ns
****
****
****
Antibody (µg/mL)
B
Undifferentiated
Relative Internalization (% of the control)
ns
ns
p = 0.0269
p = 0.0003
p = 0.0013
C
Differentiated
p = 0.0061
p = 0.0025
p = 0.0003
D
Differentiated
p = 0.0245
p = 0.0055
p = 0.0027
p = 0.0037
E
Polarized Caco-2
p = 0.0314
p = 0.0014
p = 0.0004
p = 0.0008

Figure 6

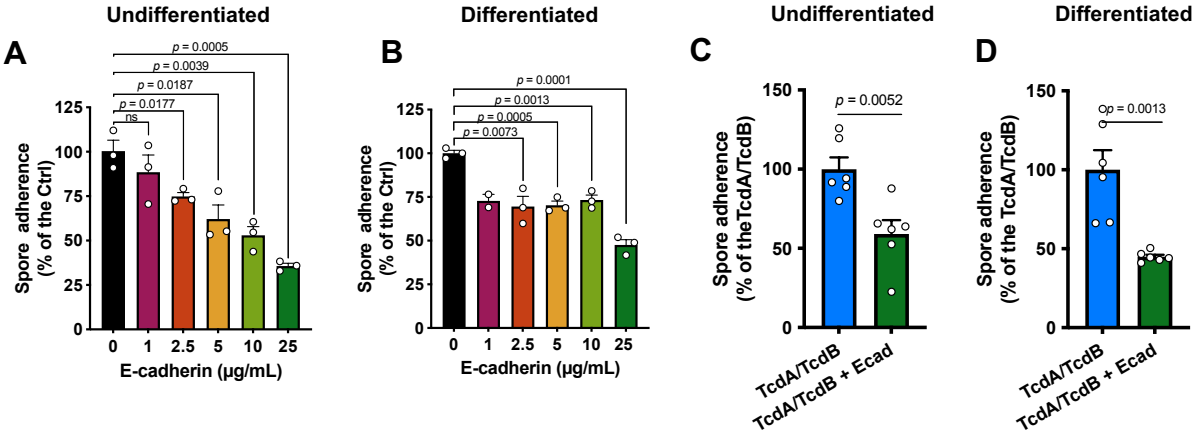
Undifferentiated
A
p = 0.0005
p = 0.0039
p = 0.0187
p = 0.0177
ns
Spore adherence (% of the Ctrl)
125
100
75
50
25
0
0
1
2.5
5
10
25
E-cadherin (µg/mL)
Differentiated
B
p = 0.0001
p = 0.0013
p = 0.0005
p = 0.0073
Spore adherence (% of the Ctrl)
E-cadherin (µg/mL)
Undifferentiated
C
p = 0.0052
Spore adherence (% of the TcdA/TcdB)
150
100
50
0
TcdA/TcdB
TcdA/TcdB + Ecad
Differentiated
D
p = 0.0013
Spore adherence (% of the TcdA/TcdB)
TcdA/TcdB
TcdA/TcdB + Ecad

Figure 7

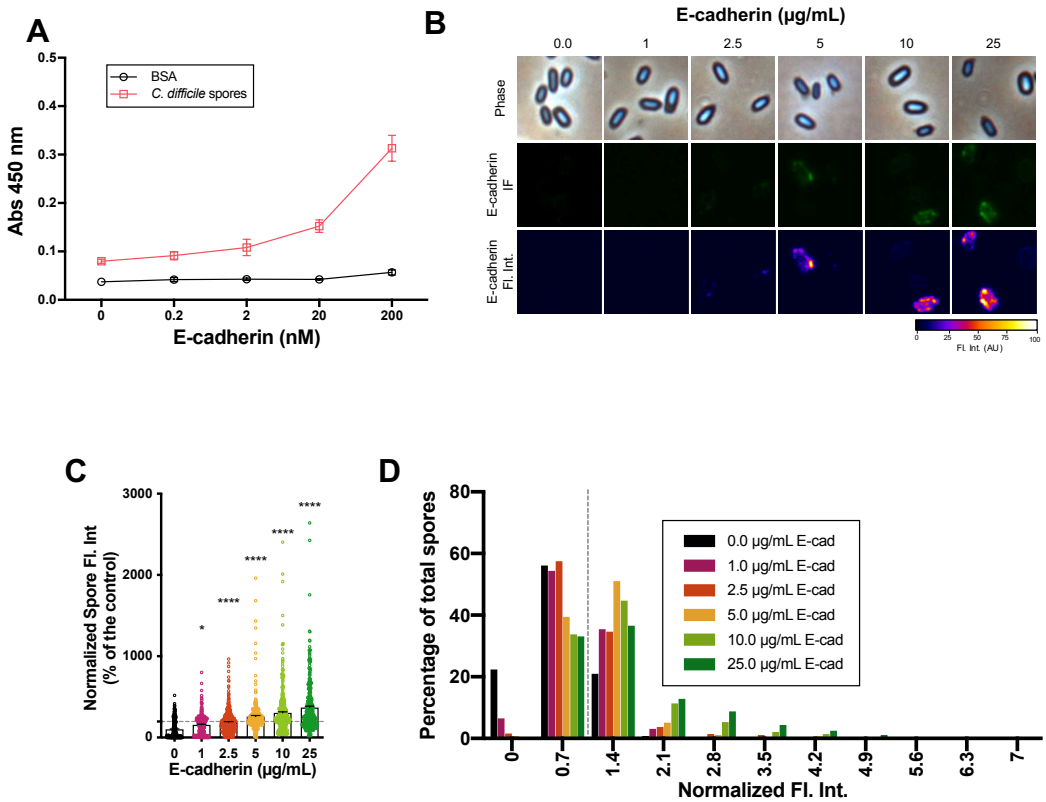
A
BSA
C. difficile spores
Abs 450 nm
E-cadherin (nM)
B
E-cadherin (µg/mL)
Phase
E-cadherin IF
E-cadherin Fl. Int.
Fl. Int. (AU)
C
Normalized Spore Fl. Int (% of the control)
E-cadherin (µg/mL)
D
Percentage of total spores
0.0 µg/mL E-cad
1.0 µg/mL E-cad
2.5 µg/mL E-cad
5.0 µg/mL E-cad
10.0 µg/mL E-cad
25.0 µg/mL E-cad
Normalized Fl. Int.

Figure 8

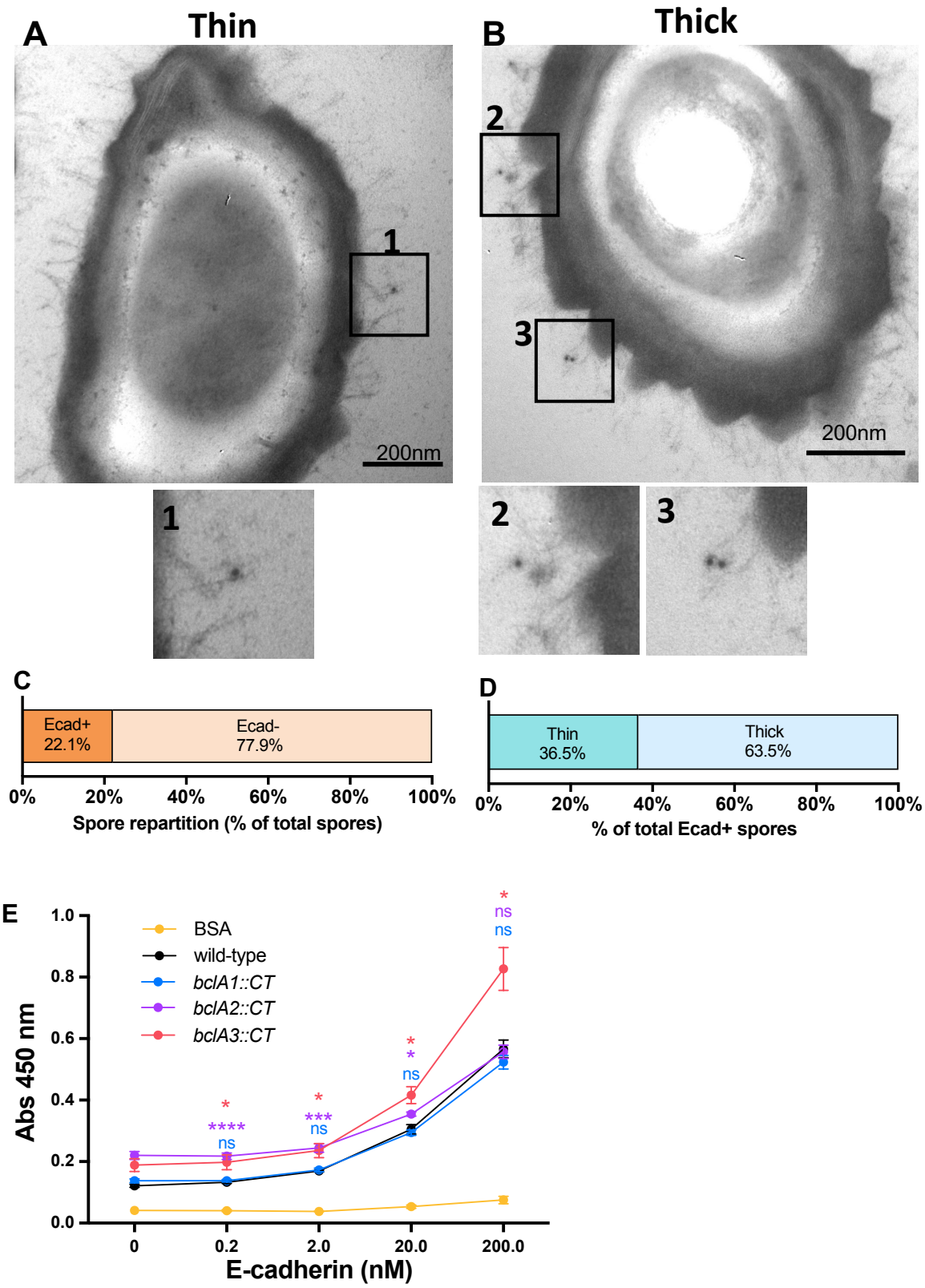
A
Thin
1
200nm
B
Thick
2
3
200nm
C
Ecad+
22.1%
Ecad-
77.9%
0%
20%
40%
60%
80%
100%
Spore repartition (% of total spores)
D
Thin
36.5%
Thick
63.5%
% of total Ecad+ spores
E
BSA
wild-type
bclA1::CT
bclA2::CT
bclA3::CT
Abs 450 nm
E-cadherin (nM)
0
0.2
2.0
20.0
200.0
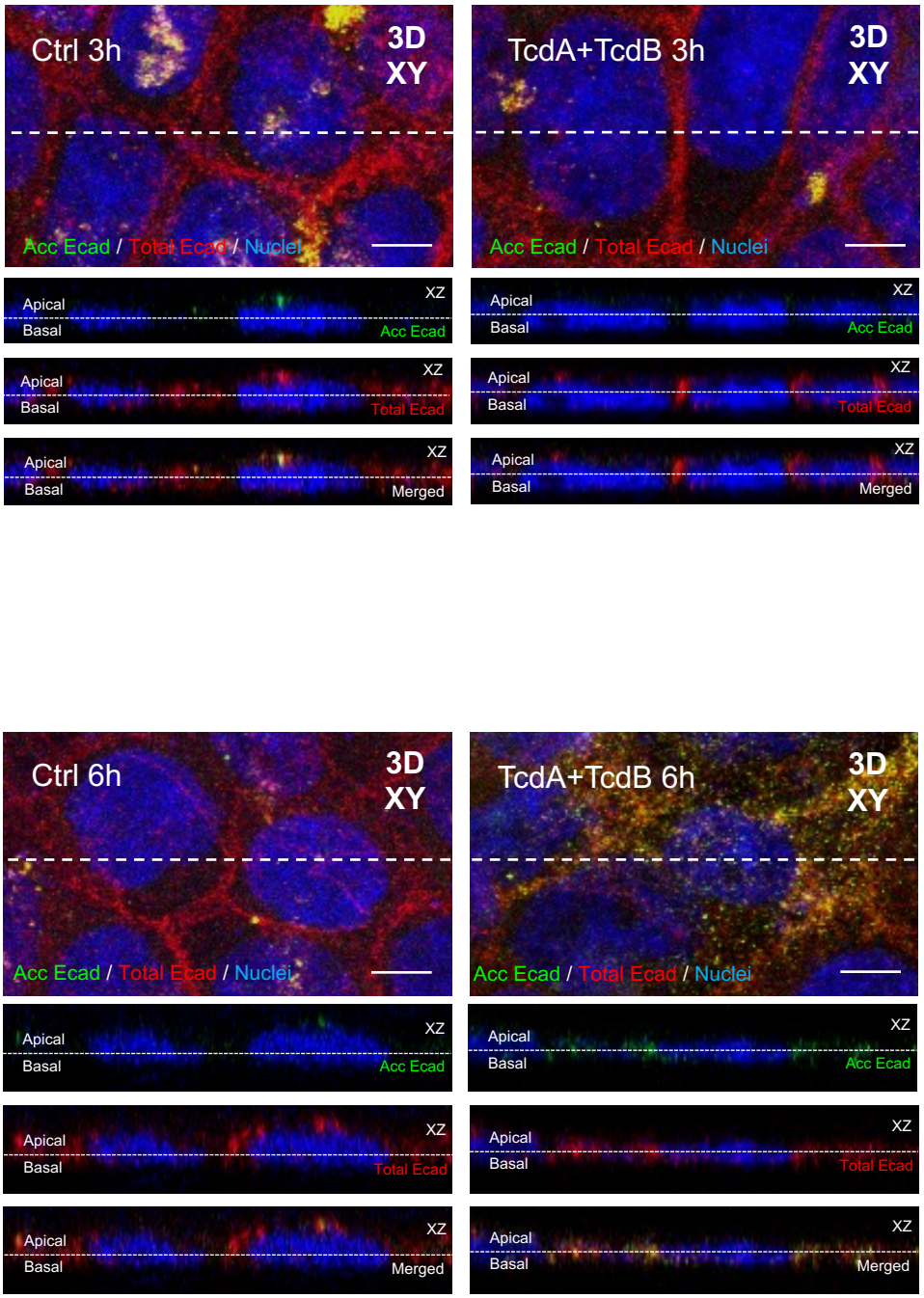
Supplementary Fig 1